RXLR-Mediated Entry of *Phytophthora sojae* Effector *Avr1b* into Soybean Cells Does Not Require Pathogen-Encoded Machinery [W]

Daolong Dou,[1] Shiv D. Kale,[1] Xia Wang, Rays H.Y. Jiang,[2] Nathan A. Bruce, Felipe D. Arredondo, Xuemin Zhang,[3] and Brett M. Tyler[4]

Virginia Bioinformatics Institute, Virginia Polytechnic Institute and State University, Blacksburg, Virginia 24061

Effector proteins secreted by oomycete and fungal pathogens have been inferred to enter host cells, where they interact with host resistance gene products. Using the effector protein Avr1b of *Phytophthora sojae*, an oomycete pathogen of soybean (*Glycine max*), we show that a pair of sequence motifs, RXLR and dEER, plus surrounding sequences, are both necessary and sufficient to deliver the protein into plant cells. Particle bombardment experiments demonstrate that these motifs function in the absence of the pathogen, indicating that no additional pathogen-encoded machinery is required for effector protein entry into host cells. Furthermore, fusion of the Avr1b RXLR-dEER domain to green fluorescent protein (GFP) allows GFP to enter soybean root cells autonomously. The conclusion that RXLR and dEER serve to transduce oomycete effectors into host cells indicates that the >370 RXLR-dEER–containing proteins encoded in the genome sequence of *P. sojae* are candidate effectors. We further show that the RXLR and dEER motifs can be replaced by the closely related erythrocyte targeting signals found in effector proteins of *Plasmodium*, the protozoan that causes malaria in humans. Mutational analysis of the RXLR motif shows that the required residues are very similar in the motifs of *Plasmodium* and *Phytophthora*. Thus, the machinery of the hosts (soybean and human) targeted by the effectors may be very ancient.

INTRODUCTION

Oomycetes are fungal-like organisms that are evolutionarily related to marine algae (Förster et al., 1990; Sogin and Silberman, 1998; Harper et al., 2005). Many oomycete species are destructive plant pathogens, including the potato late blight pathogen that caused the Irish potato famine, *Phytophthora infestans*, the Sudden Oak Death pathogen, *Phytophthora ramorum*, and the soybean root and stem rot pathogen *Phytophthora sojae* (Erwin and Ribiero, 1996). *P. sojae* alone causes $200 to $300 million in annual soybean (*Glycine max*) losses in the US and around $1 to $2 billion in losses per year worldwide (Wrather and Koenning, 2006).

Many bacterial pathogens of plants and animals deliver effector proteins into host cells using the type III secretion machinery, which consists of a pilus that transfers the proteins across the membranes of the bacteria and the host, directly into the host cytoplasm (reviewed in Staskawicz et al., 2001). Most of the disease resistance genes that protect against these pathogens

encode intracellular proteins with a nucleotide binding site–leucine-rich repeat (NBS-LRR) domain (Dangl and Jones, 2001). There are some exceptions, such as *Pto*, which encodes a protein kinase (Martin et al., 1993), and *Bs3*, which encodes a flavin monooxygenase (Romer et al., 2007). Many disease resistance genes that protect against fungal and oomycete pathogens also encode NBS-LRR proteins with a predicted intracellular location. Fungal resistance genes include the L, M, N, and P families of flax against flax rust (Lawrence et al., 1995; Anderson et al., 1997; Dodds et al., 2001a, 2001b), the rice (*Oryza sativa*) genes *Pib* (Wang et al., 1999), *Pi-ta* (Bryan et al., 2000), and Pi9 (Qu et al., 2006) against *Magnaporthe grisea*, the *Mla* resistance gene of barley (*Hordeum vulgare*) against the powdery mildew pathogen *Blumeria graminis* f. sp *hordei* (Halterman et al., 2001), the wheat (*Triticum aestivum*) *Lr1* (Cloutier et al., 2007) and *Lr10* (Feuillet et al., 2003) genes against leaf rust, and four alleles of the wheat *Pm3* gene against powdery mildew (Yahiaoui et al., 2004; Srichumpa et al., 2005).

Oomycete resistance genes include the *Arabidopsis thaliana Rpp1*, *Rpp2*, *Rpp4*, *Rpp5*, *Rpp7*, *Rpp8*, and *Rpp13* genes against *Hyaloperonospora parasitica* (Slusarenko and Schlaich, 2003), the lettuce (*Lactuca sativa*) *Dm3*, *Dm14*, and *Dm16* resistance genes against *Bremia lactucae* (Shen et al., 2002; Wroblewski et al., 2007), the potato (*Solanum tuberosum*) *R1* (Ballvora et al., 2002), *Rb* (Song et al., 2003; van der Vossen et al., 2003), and *R3a* (Huang et al., 2005) genes against *P. infestans*, and the soybean *Rps*1k (Gao et al., 2005), *Rps*4, and *Rps*6 (Sandhu et al., 2004) genes against *P. sojae*.

The predicted intracellular location of the cognate resistance gene products implies that the fungal and oomycete avirulence factors that interact with these resistance gene products must be

able to enter the cytoplasm of plant cells (Tyler, 2002). Several fungal and oomycete avirulence genes have been cloned that interact genetically with host NBS-LRR resistance genes. Most of these encode secreted proteins, including the flax rust AvrL567, AvrM, AvrP4, and AvrP123 genes (Dodds et al., 2004; Catanzariti et al., 2006), the AvrPita gene of *M. grisea* (Orbach et al., 2000), the *Avr1b*-1 gene from *P. sojae* (Shan et al., 2004), the *Avr3a* gene from *P. infestans* (Armstrong et al., 2005), and the *ATR13* (Allen et al., 2004) and *ATR1* (Rehmany et al., 2005) genes from the *Arabidopsis* downy mildew pathogen *H. parasitica*. Furthermore, in many of these cases, expression of the pathogen avirulence gene inside the host cytoplasm resulted in recognition of the avirulence proteins by the plant receptors, confirming that the cytoplasm was the site of interaction between the resistance gene products and the avirulence proteins (Allen et al., 2004; Dodds et al., 2004; Armstrong et al., 2005; Rehmany et al., 2005; Catanzariti et al., 2006). The AVR_{k1} and AVR_{a10} genes of *B. graminis* f. sp *hordei* do not encode proteins with conventional secretory leader sequences; nevertheless, the proteins trigger resistance responses when expressed in the cytoplasm of barley cells (Ridout et al., 2006). Since each of these avirulence proteins appears to enter the host cells, they have been inferred to be effector proteins. Several fungal and oomycete effector proteins that are not associated with resistance gene interactions have also been shown or inferred to enter plant cells, including *Phytophthora* elicitin (Tyler, 2002) and crinkler (Torto et al., 2003) proteins, the RTP1p protein of the bean rust *Uromyces fabae* (Kemen et al., 2005), and the ToxA protein toxin of *Pyrenophora tritici-repentis* (Manning and Ciuffetti, 2005). In all cases, the mechanisms by which these proteins might enter the cell are unknown.

The *Avr1b*-1 gene of *P. sojae* was cloned by a map-based strategy (Shan et al., 2004). It encodes a small, secreted hydrophilic protein with a mature length of 117 amino acids. The protein has no disulfide bonds. The C terminus of the protein is highly polymorphic, especially in *P. sojae* isolates that can overcome resistance provided by *Rps*1b (Shan et al., 2004). Constitutive expression of *Avr*1b in *P. sojae* transformants renders the strains unable to infect soybean cultivars containing the resistance gene *Rps*1b, and mutations in the C terminus of the protein abolish this property of *Avr1b*-1 (Dou et al., 2008). High-level constitutive expression of *Avr*1b in *P. sojae* transformants makes the strains more virulent on soybean, indicating that *Avr1b*-1 contributes positively to virulence. Avr1b proteins can suppress programmed cell death triggered in soybean, *Nicotiana benthamiana*, and *Saccharomyces cerevisiae* cells by the pro-apoptotic protein BAX, suggesting that suppression of defense-related host cell death is a mechanism by which Avr1b contributes to virulence (Dou et al., 2008).

Comparison of the sequences of the four cloned oomycete avirulence genes with each other and with large diverse families of similar genes in the *P. sojae* and *P. ramorum* genome sequences (*Avh* genes) identified two conserved motifs, termed RXLR (Arg-X-Leu-Arg) and dEER (Asp-Glu-Glu-Arg; the Asp is less well conserved than the other three residues), near the N terminus of these secreted proteins (Rehmany et al., 2005; Birch et al., 2006; Tyler et al., 2006; Jiang et al., 2008) (Figure 1). The RXLR motif closely resembles a motif (Pexel or VTF; RXLX$^E/_Q$)

that enables effector proteins of the malaria pathogen *Plasmodium* to cross the parasitiphorous vacuolar membrane into the cytoplasm of human erythrocytes (Hiller et al., 2004; Marti et al., 2004). Furthermore, one RXLR motif, that of Avr3a, was shown to function in targeting proteins from *Plasmodium* into the erythrocyte cytoplasm (Bhattacharjee et al., 2006). The structural and functional similarity between the RXLR and Pexel/VTF motifs encouraged the hypothesis that the RXLR motif was responsible for transit of the oomycete effector proteins into the cytoplasm of host cells (Rehmany et al., 2005; Birch et al., 2006; Tyler et al., 2006). Here, we experimentally verify this hypothesis by testing mutations in the RXLR and dEER motifs of the *P. sojae* Avr1b protein in both transgenic *P. sojae* and transgenic soybean tissue, supporting similar recent findings for the *P. infestans* Avr3a protein (Whisson et al., 2007). Furthermore, we demonstrate that RXLR-mediated transit does not require presence of the pathogen, indicating that transit depends only on the RXLR protein and host molecules.

RESULTS

RXLR2 and dEER Motifs of Avr1b Are Required for Its Avirulence Function in Transgenic *P. sojae* Lines

To test the function of the RXLR and dEER motifs of Avr1b, we created transgenic *P. sojae* strains that expressed either wild-type or mutant *Avr1b*-1 genes. Wild-type Avr1b contains two RXLR motifs, RXLR1 and RXLR2 (Figure 1A). We created mutations in either or both of the RXLR motifs, in addition to a mutation in the dEER motif (Figure 1A). The *Avr1b*-1 gene constructs were fused to a strong constitutive promoter, HAM34 (Judelson et al., 1991), and introduced into a strain, P7076, that expresses a variant Avr1b protein that does not confer avirulence against *Rps*1b-containing soybeans (Shan et al., 2004). Two independent transformants (T17 and T20) expressing wild-type *Avr1b*-1 (Figures 1B and 1C) lost the ability to infect soybean plants carrying *Rps*1b but were unaffected in their ability to infect plants lacking *Rps*1b (Figure 1E, Table 1). This demonstrated that they had acquired avirulence against *Rps*1b as a result of a functional Avr1b gene product. This result was confirmed using two different pairs of isolines of soybean (Buzzell et al., 1987) that differed only in the presence of *Rps*1b, namely, Williams (no *Rps* gene) with L77-1863 (*Rps*1b; Williams background) and HARO(1-7) 1 (No *Rps*; Harosoy background) with HARO13 (*Rps*1b; Harosoy background) (Figure 1E, Table 1).

By contrast, in five independent transformants expressing the RXLR2^{AAAA} mutant, there was no gain of avirulence against *Rps*1b cultivars, despite the presence of abundant mRNA from the transgene (Figure 1E, Table 1). Thus, the RXLR2 motif is necessary for Avr1b activity when the protein is delivered by the pathogen. Since the RXLR1 motif was intact in the RXLR2^{AAAA} mutant, the motif appeared to be nonfunctional. Consistent with this inference, the RXLR1^{AAAA} mutation did not abolish avirulence in three independent transformants (Figure 1E, Table 1). As expected, avirulence was lost in the RXLR1^{AAAA} RXLR2^{AAAA} double mutants (Figure 1E, Table 1). A mutation in the dEER motif also abolished avirulence (in two independent transformants),

Figure 1. RXLR and dEER Motifs Are Required for Avr1b Function in *P. sojae* Transformants.

(A) Sequences of mutations in the RXLR1, RXLR2, and dEER motifs. Blue represents wild-type amino acids targeted for replacement by Ala residues (red).

(B) *Pst*I restriction analysis of PCR products amplified from *Avr1b*-1 transformants using primers specific for the HAM34 promoter and terminator regions. *Pst*I restriction profiles of Avr1b(RXLR1AAAA), Avr1b(RXLR2AAAA), Avr1b(RXLR1AAAA, 2AAAA), Avr1b(dEERA6), and wild-type Avr1b are distinguished from each other because the mutations introduce a *Pst*I site. Avr1b(dEERA6)-9 was confirmed by sequencing the PCR product.

(C) Detection of Avr1b mRNA in *P. sojae* stable transformants by RT-PCR. Top panel shows amplification with primers internal to the Avr1b C terminus. Bottom panel shows amplification with *P. sojae* actin primers. *P. sojae* stable transformants were the same as for **(B)** except that an amplification reaction is also shown from RNA from a *P. sojae* transformant containing a GUS gene. No amplification was observed when reverse transcriptase was omitted from the reactions.

(D) Distributions of HMM scores of RXLR flanking regions for all RXLR-containing secreted proteins from *P. sojae* and *P. ramorum* (nonpermuted), for all secreted proteins retaining an RXLR string after sequence permutation (permuted), and for all high-quality RXLR-effector candidates identified by Jiang et al. (2008) (curated). The locations on the distribution of the HMM scores of the RXLR strings of known avirulence proteins and HpAvh341 are shown by the arrows.

(E) Phenotype of L77-1863 (*Rps*1b) seedlings inoculated on the hypocotyls with transformants carrying the indicated wild-type or mutant *Avr1b*-1 genes and photographed 4 d later.

indicating that this motif is also required for the function of the protein (Figure 1E, Table 1).

The difference in activity between RXLR1 and RXLR2 suggests that surrounding sequences are important to the activity of an RXLR motif. To define the differences in the surrounding sequences, we created a hidden Markov model (HMM) using the 10–amino acid residues to the left and right of the RXLR motifs of all of the *P. sojae* and *P. ramorum* Avh genes (Tyler et al., 2006;

Jiang et al., 2008). Using this HMM, the sequences surrounding RXLR2 had a high score of 18.5, representing an excellent match to the consensus flanking sequence, very unlikely to have been found in a random sequence. By contrast, sequences surrounding RXLR1 had a low, nonsignificant score of 0.0. Using the same HMM, the sequences surrounding the RXLR motif of *P. infestans* Avr3a scored 10.9. Using a similar HMM derived from *H. parasitica* Avh genes, the sequences surrounding the RXLR motifs of

Table 1. Molecular Characterization and Avirulence Testing of *P. sojae* Stable Transformants

Strains	Transgene (PCR)[a]	Expression (RT-PCR)[b]	Transformant Validation[c]	Avirulence (Surviving Seedlings)[d]		P[e]
				*Rps*1b	*rps*	
P7076 (GUS)						
GUS	−	−		1/23	1/22	0.77
P7076 (s*Avr1b* WT)						
T17	+	+	*Pst*I	20/30	0/21	3.9 E-07
T20	+	+	Sequence	25/44	2/28	1.2 E-05
P7076 (s*Avr1b* RXLR1^AAAA)						
RXLR1-2	+	+	*Pst*I	32/36	3/20	5.0 E-08
RXLR1-3	+	+	*Pst*I	31/54	3/21	6.4 E-04
RXLR1-5	+	+	*Pst*I	37/57	7/23	5.1 E-03
P7076 (s*Avr1b* RXLR2^AAAA)						
RXLR2-18	+	+	*Pst*I	6/44	3/17	0.48
RXLR2-20	+	+	*Pst*I	4/46	3/19	0.33
P7076 (s*Avr1b* RXLR1^AAAA; RXLR2^AAAA)						
RXLR1+2-4	+	+	*Pst*I	5/31	2/16	0.55
RXLR1+2-6	+	+	*Pst*I	4/43	1/21	0.47
P7076 (s*Avr1b* dEER^A6)						
dEER-9	+	+	Sequence	4/59	2/23	0.79
dEER-14	+	+	*Pst*I	4/40	3/15	0.28
Ps *Avr4/6-Avr1bCt*						
4/6-1b-3	+	+	Size	15/24	3/11	0.057
4/6-1b-19	+	+	Size	14/26	3/16	0.025
Hp *341-Avr1bCt*						
341-1b-13	+	+	Size	16/19	0/11	6.6 E-06
341-1b-17	+	+	Size	23/24	0/7	3.0 E-06
mAvr1bCt						
mAvr1bCt-4	+	+	Size	3/20	3/16	0.77
mAvr1bCt-5	+	+	Size	2/21	1/15	0.63

[a] The presence of transgenes was verified by PCR as described in Methods. +, transgene present; − transgene not detected.

[b] Transgene expression was determined by qualitative RT-PCR and by quantitative RT-PCR as described in Methods. +, transgene transcripts present; −, transgene transcripts not detected.

[c] The presence of the relevant mutation in the transforming plasmid was verified by sequencing in every case. The presence of the correct mutation within the transgenes of each transformed strain was verified after PCR amplification of the *Avr1b*-1 transgene by *Pst*I digestion, by sequencing in the case of the mutants (e.g., Figure 1), or by size in the case of the Avh gene fusions and N-terminal deletion (e.g., Figure 4).

[d] The avirulence of each transgenic strain was tested by inoculation of seedlings containing *Rps*1b (L77-1863) or no *rps* gene (Williams) as described in Methods. The number of surviving seedlings/total inoculated seedlings is shown, summed from all replicates

[e] Fisher's exact test (one tailed) was used to compare the frequency of seedling survival between *rps* and *Rps*1b plants. A significant P value (0.05) indicates that the transformant's phenotype is avirulent.

the *H. parasitica* Atr1 and Atr13 proteins had scores of 9.8 and 6.3, respectively.

To establish the significance of these HMM scores, we used the *Phytophthora* HMM to score the RXLR motifs of 1240 RXLR-containing sequences identified from a pool of all putative secreted *P. sojae* and *P. ramorum* proteins by Jiang et al. (2008). As a control, we scored 639 RXLR-containing sequences found after permuting the sequences of all the putative secreted *P. sojae* and *P. ramorum* proteins (Jiang et al., 2008). As shown in Figure 1D, the RXLR strings of 698 (56%) of the 1240 real proteins had an HMM score of zero, while the RXLR strings of 595 (93%) of the permuted proteins had a zero score, and only 13 (1.8%) scored above 5.0. By contrast, of 765 proteins that Jiang et al. (2008) identified as high-quality candidate effectors, only 18% had an HMM score of zero, and 543 (72%) had a score >5.0.

From this comparison, we conclude that HMM scores of zero, such as that of Avr1b RXLR1, are characteristic of RXLR strings found at random, while scores >5.0 are characteristic of non-random occurrences of RXLR strings and of the RXLR strings of functional avirulence proteins. HMM scores between 0 and 5 are equivocal. The curated Avh genes with a score of zero may represent pseudogenes as many of them were identified principally by C-terminal sequence similarity.

The Interaction between Avr1b and the *Rps*1b Gene Product Occurs within Host Cells and Does Not Require the RXLR and dEER Motifs

To confirm that the site of interaction of Avr1b with the *Rps*1b gene product is within plant cell, we used particle bombardment

to introduce DNA encoding Avr1b proteins lacking a secretory leader into soybean cells together with DNA encoding β-glucuronidase (GUS). This assay measures the functional interaction of the Avr1b protein with the intracellular product of the soybean *Rps*1b gene; when the two proteins interact, programmed cell death is triggered in the transformed cells ablating the development of tissue patches expressing GUS (Mindrinos et al., 1994; Qutob et al., 2002). Since the Avr1b protein lacks its normal secretory leader, the protein should be synthesized in the plant cytoplasm. To facilitate the comparison of test and control bombardments, we used a novel double-barreled attachment for the Bio-Rad Gene Gun (Dou et al., 2008) that enables us to shoot two different DNA samples side by side into a leaf in the same shot, which greatly improves the reproducibility of the results (Dou et al., 2008). Figure 2 shows that delivery of DNA encoding leaderless Avr1b protein into soybean cells significantly reduced the number of blue GUS-positive patches when the *Rps*1b gene was present but not when *Rps*1b was absent (Figure 2A). This is consistent with a cytoplasmic location for the Avr1b–Rps1b interaction. When RXLR2 or dEER motifs were replaced by four or six Ala residues, respectively [Figure 2A, mAvr1b(RXLR2^{AAAA}) and mAvr1b(dEER^{A6})], the interaction of the cytoplasmic, leaderless Avr1b with Rps1b was unaffected (Figures 2A and 2B), indicating that the RXLR2 and dEER motifs were not required for the interaction.

RXLR-Mediated Transit into Soybean Cells Does Not Require the Pathogen

To test whether RXLR function requires the presence of the pathogen, we used the bombardment assay to determine the effect of the RXLR2^{AAAA} mutation on secreted Avr1b protein. When soybean cells were bombarded with DNA encoding wild-type Avr1b, including its normal secretory leader, a reduction in GUS-positive blue spots was observed comparable to that observed for the nonsecreted protein [Figure 2A, sAvr1b(WT)]. However, when the RXLR2^{AAAA} or dEER^{A6} mutations were present in the bombarded DNA, there was no reduction in the number of blue spots [Figure 2A, sAvr1b(RXLR2^{AAAA}) and sAvr1b (dEER^{A6})]. Figure 2C shows a leaf bombarded simultaneously side by side with the sAvr1b(WT) and sAvr1b(RXLR2^{AAAA}) constructs, illustrating the reduction observed with the wild-type construct compared with the mutant. From these results, we infer first that the secretory leader is functional in soybean and targets Avr1b protein to the outside of the cell. Second, we infer that the RXLR2 (but not RXLR1) and dEER motifs are required for Avr1b protein to reenter the cell, which confirms the conclusion from the *P. sojae* transformation experiments. Importantly, the results also show that RXLR-dEER–mediated entry does not require the presence of the pathogen.

To support our inference that the secretory leader of Avr1b was correctly exporting the protein from the plant cells in the bombardment assay, we constructed a gene encoding *Aequorea coerulescens* green fluorescent protein (acGFP; abbreviated GFP in this article) fused either to the Avr1b leader or to full-length Avr1b. These fusions enabled us to track the proteins and check their stability. To aid in visualization, we used onion bulb epidermal cells for these experiments rather than soybean cells.
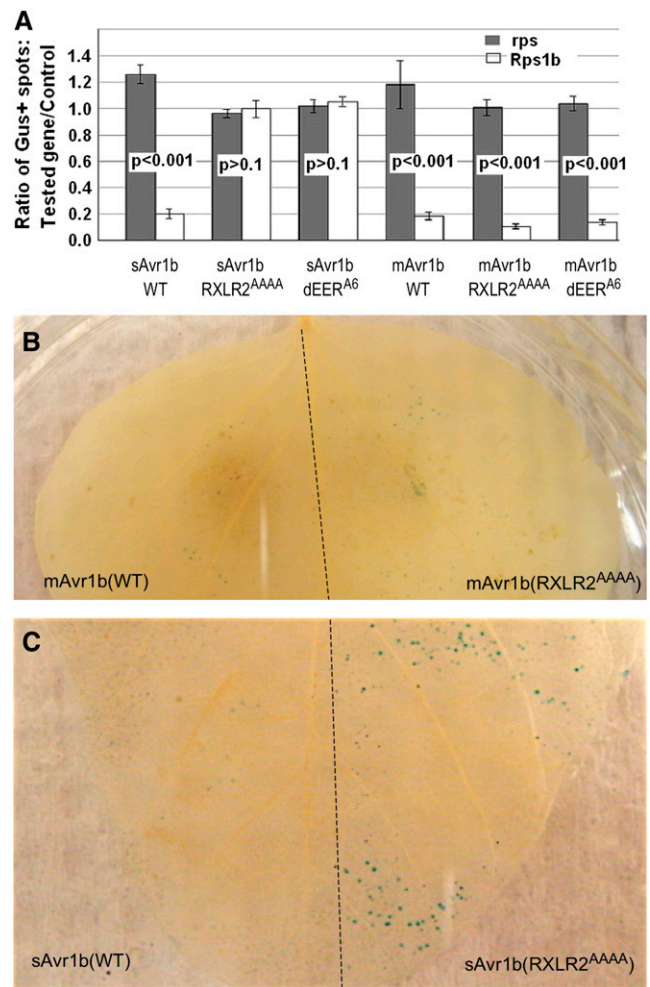

Figure 2. RXLR and dEER Functions Confirmed by Particle Bombardment Assay.

Soybean leaves were bombarded using a double-barreled device that delivered *Avr1b*-1 DNA-bearing particles to one side of the leaf and control (empty vector) DNA to the other; both sides received GUS DNA. **(A)** Ratio of blue spots in the presence of *Avr1b*-1 compared with the control. sAvr1b indicates a gene encoding secretory Avr1b, and mAvr1b indicates one encoding mature Avr1b (lacking the secretory leader). WT indicates wild-type RXLR motif, RXLR2^{AAAA} indicates the four Ala replacement of the RXLR2 motif, and dEER^{A6} indicates the six Ala replacement of the dEER motif. Averages and SE are from 16 pairs of shots. P values comparing results from cultivars with *Rps*1b (L77-1863) or without (rps; Williams) were calculated using the Wilcoxon rank sum test.
(B) Direct comparison of bombardment with mature Avr1b.
(C) Direct comparison of bombardment with secretory Avr1b.
In both **(B)** and **(C)**, DNA encoding wild-type (left) and RXLR2^{AAAA} (right) versions of mAvrb or sAvr1b, respectively, were bombarded onto the same leaf of L77-1863 (*Rps*1b). The dashed lines indicate the positions of a divider that prevents particles from the two shots from overlapping. In both photographs, the brightness and contrast were adjusted uniformly to improve the visibility of the blue spots.

GFP was exported from the cells and accumulated in the apoplast when the secretory leader was attached to GFP (Figure 3A) but accumulated in the cytoplasm and nucleus when the leader was not attached (Figure 3B), as has been observed by others (e.g., Bonello et al., 2002; Yamane et al., 2005). When full-length Avr1b was fused to GFP, the proteins also accumulated in the apoplast if a mutation was present in either the RXLR2 motif (Figure 3C) or in the dEER motif (Figure 3D). This observation confirmed that the protein encoded by these mutants was stable and correctly targeted outside of the cells. When cells expressing Avr1b-GFP fusion proteins with RXLR mutations were plasmolyzed by treatment with 0.8 M mannitol for 15 min, the GFP was
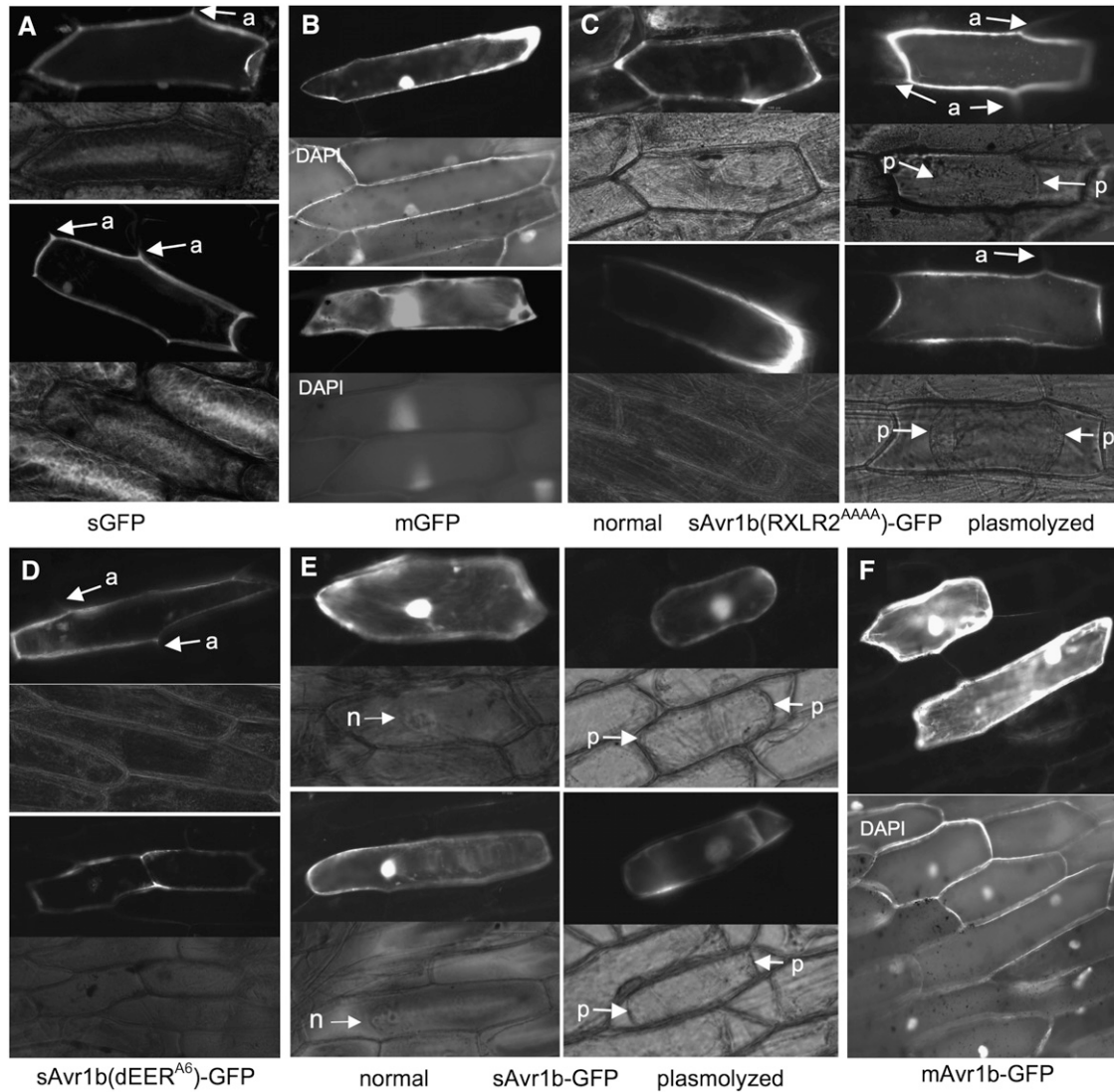
Figure 3. Secretion and Reentry of Avr1b-GFP Fusion Proteins Expressed in Onion Cells.

DNA encoding various fusions of Avr1b with *A. coerulescens* GFP was bombarded into onion epidermal cells using the Gene Gun without the double-barrel attachment. Cells were photographed under both UV and white light illumination 12 to 24 h after bombardment. a, sites where secreted GFP has begun to spread into the apoplast between pairs of neighboring cells; n, nuclei visualized under white light; p, plasma membrane in plasmolyzed cells; DAPI, cells stained with 4′,6-diamidino-2-phenylindole and photographed under UV illumination.
(A) Fusion of GFP to the secretory leader of Avr1b alone.
(B) GFP with no secretory leader (native GFP). DAPI-stained cells are shown instead of white light–illuminated cells.
(C) GFP fused to the Avr1b RXLR2[AAAA] mutant, including its secretory leader. In the top right panel, a white trace of the plasma membrane from the panel below has been added. The right-side panels show photographs of plasmolyzed cells.
(D) GFP fused to Avr1b dEER[A6] mutant, including its secretory leader.
(E) GFP fused to wild-type Avr1b, including its secretory leader. The right-side panels show photographs of plasmolyzed cells.
(F) GFP fused to mature Avr1b lacking its secretory leader. DAPI-stained cells are shown instead of white light–illuminated cells.

associated with the cell wall and not with the plasma cell membrane (Figure 3C, right panels; see Supplemental Figure 1 online). Furthermore, GFP protein could be seen diffusing into the apoplast between pairs of neighboring cells (arrows marked by "a" in Figures 3A, 3C, and 3D). Similar observations were made when cells expressing secreted GFP or Avr1b-GFP fusion proteins with a dEER mutation were plasmolyzed (see Supplemental Figure 1 online). If the RXLR2 and dEER motifs were intact, however, the sAvr1b-GFP protein fusion accumulated in the cytoplasm and nucleus of the cells (Figure 3E), similar to the mAvr1b-GFP fusion lacking the leader (Figure 3F). When cells expressing sAvr1b-GFP fusion proteins were plasmolyzed by treatment with 0.8 M mannitol for 15 min, the GFP could be observed to have either fully or partially returned to the inside of the cells (Figure 3E, right panels). These results supported our conclusion that the RXLR2 and dEER motifs act together to enable Avr1b protein to reenter the plant cells.

The Avr1b RXLR and dEER Motifs Are Sufficient to Target GFP to Soybean Cells

Shan et al. (2004) showed that culture filtrates of *Pichia pastoris* cells secreting Avr1b proteins could trigger the hypersensitive response in soybean leaves expressing the *Rps*1b resistance gene. Subsequently, it proved extremely difficult to consistently produce enough soluble Avr1b protein in *P. pastoris* or any other expression system to repeat this observation. As an alternative, we fused the RXLR-dEER region of Avr1b to GFP, synthesized the fusion protein in *Escherichia coli*, and partially purified it (Figure 4A). Root tips of soybean seedlings were incubated with the isolated fusion protein for 12 h, washed for 4 h in water, and then observed under light and UV microscopy to localize the GFP. As shown in Figure 4C, GFP accumulated inside many of the root cells, whereas buffer alone did not produce any fluorescence (Figure 4B). The optical sections produced by the confocal microscope (Figure 4C) revealed that the protein penetrated ~10 cell layers deep during the 12-h incubation. The characteristic accumulation of GFP in the nuclei of the treated cells (Figure 4G) is comparable to the pattern observed when GFP is expressed in planta (Figures 3B, 3E, and 3F) and verifies that the GFP is located inside the cells. The nuclear localization of the protein also indicates that the cells are alive. If mutations were present in the RXLR or dEER motifs of the fusion protein, GFP did not accumulate inside the soybean root cells (Figures 4E and 4F, respectively). When the RXLR-dEER region was replaced by the artificial protein transduction motif Arg_9 (Chang et al., 2005, 2007; see below), GFP once again entered the soybean root cells (Figure 4E) and accumulated in the nuclei (Figure 4H).

Avr1b RXLR and dEER Motifs Can Be Replaced by RXLR-dEER–Containing Protein Sequences Encoded by Bioinformatically Identified Avh Genes

To determine if the RXLR and dEER motifs of bioinformatically identified *Avh* genes could functionally replace the RXLR2 and dEER motifs of *Avr1b*-1, we fused full-length *Avh* genes from *P. sojae* and *H. parasitica* to an *Avr1b*-1 N-terminal deletion mutant lacking the RXLR and dEER motifs. The fusion genes were then introduced into *P. sojae*, and the transformants were tested for avirulence on *Rps*1b-containing soybean cultivars. Both *Avh* genes, *P. sojae Avh*171 (since identified as Avr4/6; Dou et al., 2008) and *H. parasitica Avh*341, could replace the requirement for the RXLR2 and dEER motifs as judged by the avirulence of the transformants on *Rps*1b-containing cultivars, whereas transformants containing only the C terminus of Avr1b fused to an initiator Met remained virulent (Figure 5, Table 1). This result indicates that the RXLR and dEER motifs form a distinct transferable functional domain of Avr1b and other Avh proteins. The HMM scores of the RXLR-dEER motifs of Ps Avr4/6 and Hp Avh341 are both well within the functional range (6.9 and 14.2, respectively) (Figure 1D).

The Avr1b Host Targeting Signal Can Be Functionally Replaced by Autonomous Protein Transduction Motifs

Protein transduction domains (PTDs) capable of autonomously carrying proteins across plasma cell membranes have been described and characterized in the HIV-1 Tat protein (Joliot, 2005). Arg-rich peptides such as Arg_9 can also perform this function (Futaki, 2002). To compare RXLR-dEER–mediated effector delivery with the function of PTDs, we replaced the RXLR2 motif of Avr1b with TAT PTD or with Arg_9 (Figure 6A). When we tested the resultant proteins using the particle bombardment assay, both PTDs could functionally replace the RXLR2 motif of Avr1b, restoring the avirulence reaction of Avr1b with Rps1b (Figure 6B). Furthermore, when we fused the version of secreted Avr1b that contained the Arg_9 sequence in place of the RXLR2 motif to GFP, the fusion protein accumulated in the cytoplasm and the nucleus of bombarded onion bulb cells rather than the apoplast, confirming that Arg_9 could functionally replace RXLR2 (Figure 6C). Similar results were obtained when we fused the version of secreted Avr1b that contained the TAT PTD in place of the RXLR2 motif to GFP (Figure 6D). Finally, when Arg_9 was fused to GFP, the isolated proteins could enter soybean root cells directly (Figures 4D and 4H), as also observed for onion root cells (Chang et al., 2005). TAT PTD-GFP fusion proteins also could enter onion root cells (Chang et al., 2005).

The Avr1b Host Targeting Signal Is Interchangeable with Host Targeting Signals from *Plasmodium* Effectors

To test if the erythrocyte targeting signals of *Plasmodium* effector proteins could functionally replace the RXLR-dEER region of Avr1b, we replaced the residues of Avr1b from the end of the secretory leader to the end of the dEER motif with the mature N termini of three different *Plasmodium* effector proteins that are targeted to the erythrocyte cytoplasm, namely, PfGBP-130, PfHRPII, and PfPFE1615c (Bhattacharjee et al., 2006). The entire 37– to 41–amino acid region of each *Plasmodium* effector required for transduction (Bhattacharjee et al., 2006) was used (Figure 6A). As shown in Figure 6B, all three *Plasmodium* host targeting domains could functionally replace the Avr1b N terminus in targeting Avr1b to the soybean cytoplasm, assuming that they do not simply interfere with secretion.
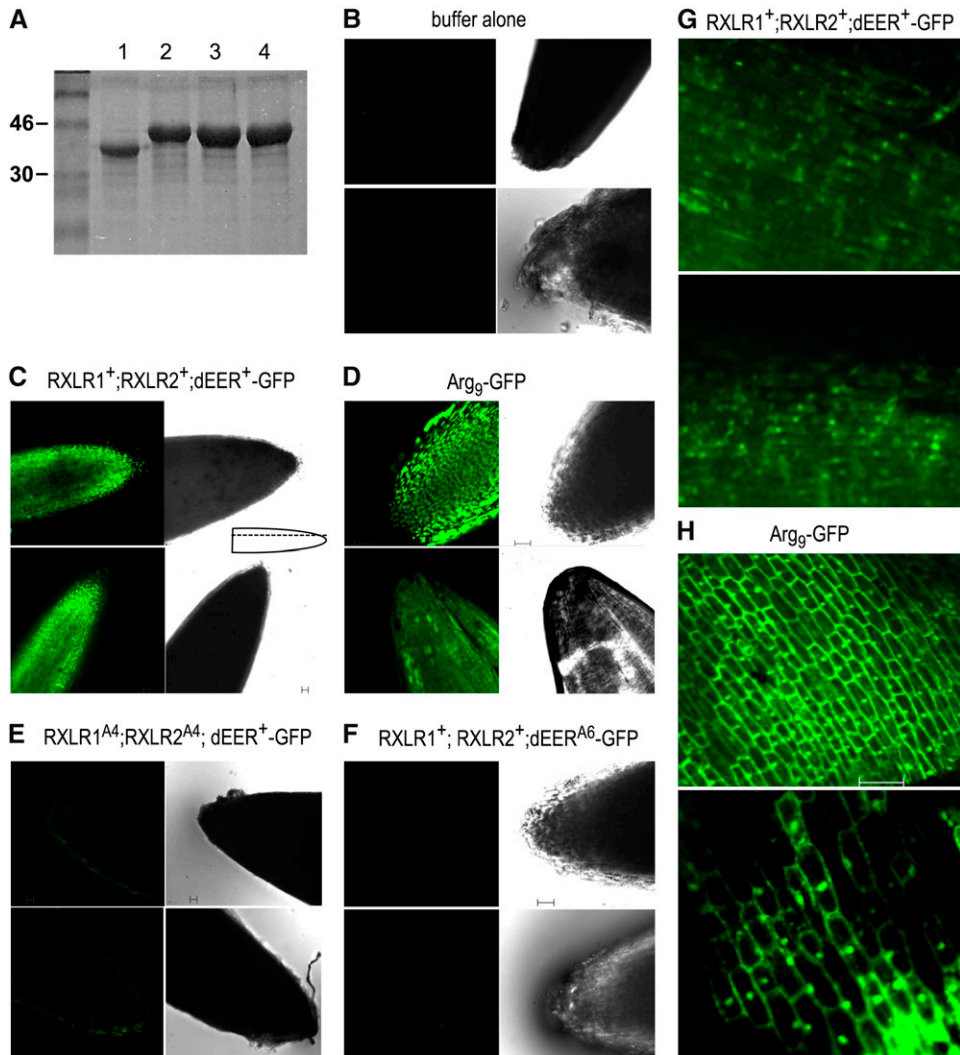
Figure 4. RXLR-dEER-GFP Fusion Proteins Isolated from *E. coli* Can Enter Soybean Cells in the Absence of the Pathogen.

GFP fusion proteins were expressed in *E. coli*, partially purified, and incubated with soybean root tips for 12 h. The root tips were then washed for 4 h and photographed under UV and white light illumination.

(A) Protein gel electrophoresis analysis of GFP fusion proteins partially purified from *E. coli* cells: lane 1, Arg_9-GFP; lane 2, GFP fused to the N-terminal 44 amino acids of mature wild-type Avr1b protein ($RXLR1^+,RXLR2^+$-dEER-GFP); lane 3, same as lane 2 with both RXLR1 and RXLR2 mutations ($RXLR1^{AAAA},RXLR2^{AAAA}$-dEER-GFP); lane 4, same as lane 2 except with dEER mutation ($RXLR1^+,RXLR2^+$-$dEER^{AAAAAA}$-GFP). The left lane contained molecular mass markers; the sizes of the markers are shown on the left (in kD). All expressed GFP proteins fluoresce normally under UV illumination.

(B) to **(F)** UV (left panels) and back-lit white light (right panels) illumination of roots after incubation with the indicated GFP protein fusion. The UV photographs represent longitudinal optical sections taken using the confocal microscope as illustrated by the dashed line in the inset of **(C)**. The GFP concentration, illumination, and exposure of the UV photographs was identical in all 10 panels shown.

(B) Buffer alone with no fusion protein.

(C) $RXLR1^+,RXLR2^+$-dEER-GFP.

(D) Arg_9-GFP.

(E) $RXLR1^{AAAA},RXLR2^{AAAA}$-dEER-GFP.

(F) $RXLR1^+,RXLR2^+$-$dEER^{AAAAAA}$-GFP.

(G) and **(H)** Higher-magnification photographs after the root tips were gently squashed following washing, showing nuclear accumulation of GFP.
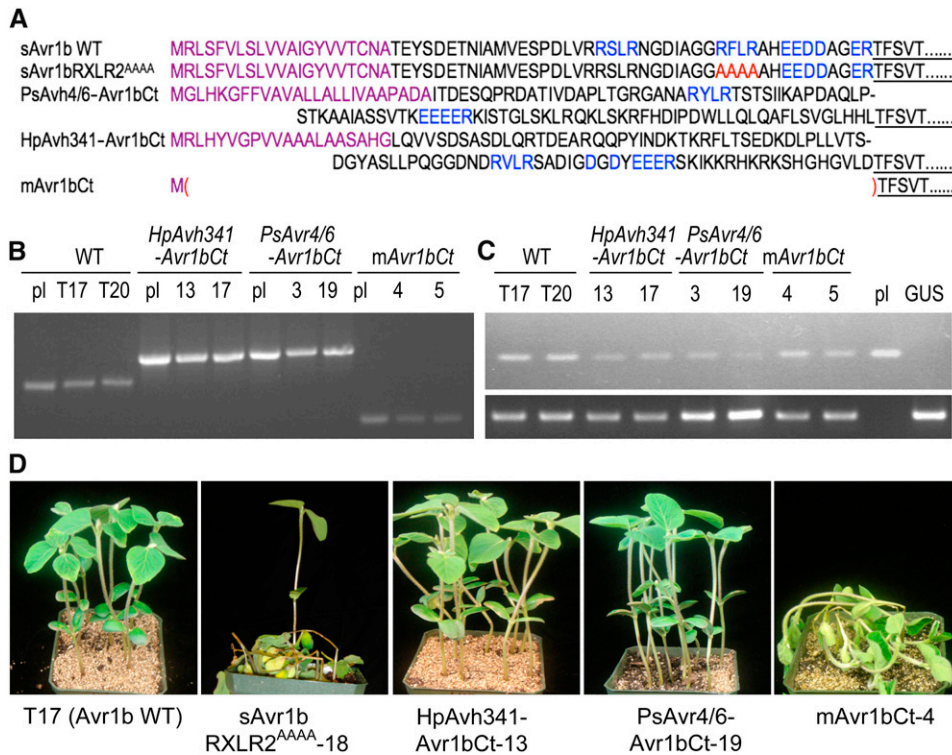
(G) $RXLR1^+,RXLR2^+$-dEER-GFP.

(H) Arg_9-GFP.

A

```
sAvr1b WT          MRLSFVLSLVVAIGYVVTCNATEYSDETNIAMVESPDLVRRSLRNGDIAGGRFLRAHEEDDAGERTFSVT......
sAvr1bRXLR2^AAAA   MRLSFVLSLVVAIGYVVTCNATEYSDETNIAMVESPDLVRRSLRNGDIAGGAAAAAHEEDDAGERTFSVT......
PsAvh4/6-Avr1bCt   MGLHKGFFVAVALLALLIVAAPADAITDESQPRDATIVDAPLTGRGANARYLRTSTSIIKAPDAQLP-
                   STKAAIASSVTKEEEERKISTGLSKLRQKLSKRFHDIPDWLLQLQAFLSVGLHHLTFSVT......
HpAvh341-Avr1bCt   MRLHYVGPVVAAALAASAHGLQVVSDSASDLQRTDEARQQPYINDKTKRFLTSEDKDLPLLVTS-
                   DGYASLLPQGGDNDRVLRSADIGDGDYEEERSKIKKRHKRKSHGHGVLDTFSVT......
mAvr1bCt           M(                                                                  )TFSVT......
```

B

C

D

T17 (Avr1b WT) | sAvr1b RXLR2^AAAA-18 | HpAvh341-Avr1bCt-13 | PsAvr4/6-Avr1bCt-19 | mAvr1bCt-4

Figure 5. *P. sojae* Stable Transformants Show That Two Other Avh Proteins Can Replace the RXLR-dEER Region of Avr1b.

(A) Sequences of the N termini of wild-type and mutant Avr1b proteins and of fusions with two other Avh proteins. Purple, secretory leader; blue, RXLR motif; red, dEER motif. The C-terminal sequence of Avr1b is underlined.
(B) PCR analysis of DNA from *P. sojae* stable transformants. WT: pl, pHamAvr1b plasmid DNA; T17 and T20, two transformants with wild-type *Avr1b*-1 transgenes. *HpAvh341-Avr1bCt*: pl, pHamAvh341 plasmid DNA (encoding Hp Avh341-Avr1bCt); 13 and 17, two transformants containing pHamAvh341. PsAvr4/6-Avr1bCt: pl, pHamAvh171 plasmid DNA (encoding Ps Avr4/6-Avr1bCt); 3 and 19, two transformants containing pHamAvh171. *mAvr1bCt*: pl, pHamAvr1bCt plasmid DNA (encoding mAvr1bCt protein); 4 and 5, two transformants containing pHamAvr1bCt. The sizes of the PCR products for *Avr1b*-1, pHamAvh341, pHamAvh171, and pHamAvr1bCt are 577, 721, 748, and 385 bp, respectively.
(C) Detection of Avr1b mRNA in *P. sojae* stable transformants by RT-PCR. Top panel shows amplification with primers internal to the Avr1b C terminus. Bottom panel shows amplification with *P. sojae* actin primers. *P. sojae* stable transformants were the same as for **(B)** except that an amplification reaction is also shown from RNA from a *P. sojae* transformant containing GUS. Pl, pHamAvr1b plasmid DNA as template. No amplification was observed when reverse transcriptase was omitted from the reactions.
(D) Phenotype of L77-1863 (*Rps*1b) seedlings inoculated on the hypocotyls with the indicated transformants carrying wild-type or mutant *Avr1b*-1 genes and photographed 4 d later. HpAvh341-Avr1b-17, PsAvr4/6-Avr1b-3, and mAvr1bCt-5 gave similar results to HpAvh341-Avr1b-13, PsAvr4/6-Avr1b-19, and mAvr1bCt-4 (Table 1).

Functional Characterization of the RXLR Motif

To begin to experimentally characterize the sequence requirements of the RXLR motif, we introduced a series of mutations into the motif in a version of the *Avr1b*-1 gene that retained the secretory leader and assayed the mutants using the bombardment assay (Table 2). Mutations that targeted the Arg at position 1 or the Leu at position 3 have the strongest effect on the ability of Avr1b to ablate GUS-positive tissue patches. Replacement of R1 with Lys reduced function significantly (33% ablation compared with 78%; $P < 0.001$), while Gln replacement completely abolished it. Replacement of L3 with Ala or even the relatively conservative Val also completely abolished function. Replacement of the Arg at position 4 with a Gln slightly but significantly reduced function (58% ablation compared with 72%; $P < 0.001$).

Reversing the order within the first and second two pairs of positively charged and hydrophobic residues (RFLR → FRLR; RFLR → RFRL) completely abolished avirulence activity, indicating that positions of R1 and L3 were critical, not just their presence.

DISCUSSION

Since many resistance genes against oomycetes encode intracellular proteins and since several cognate oomycete avirulence genes encode secreted proteins, it has been inferred that there must be a mechanism for translocating the avirulence proteins into the plant cells (Tyler, 2002; Allen et al., 2004; Armstrong et al., 2005; Rehmany et al., 2005). Since the RXLR and dEER
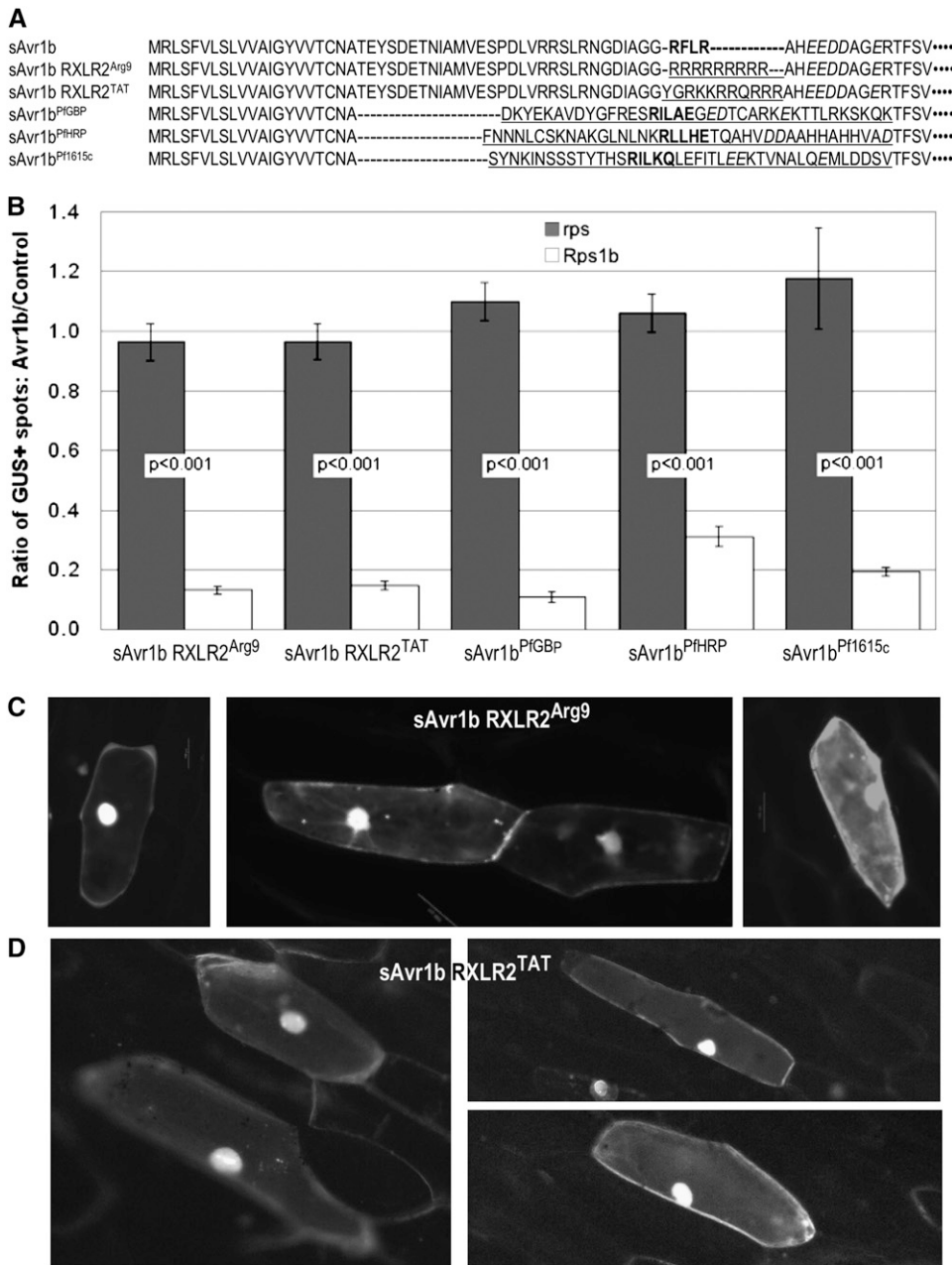
A

sAvr1b	MRLSFVLSLVVAIGYVVTCNATEYSDETNIAMVESPDLVRRSLRNGDIAGG-**RFLR**------------AH*EEDD*AGERTFSV••••
sAvr1b RXLR2^{Arg9}	MRLSFVLSLVVAIGYVVTCNATEYSDETNIAMVESPDLVRRSLRNGDIAGG-<u>RRRRRRRRR</u>---AH*EEDD*AGERTFSV••••
sAvr1b RXLR2^{TAT}	MRLSFVLSLVVAIGYVVTCNATEYSDETNIAMVESPDLVRRSLRNGDIAGG<u>YGRKKRRQRRRA</u>H*EEDD*AGERTFSV••••
sAvr1b^{PfGBP}	MRLSFVLSLVVAIGYVVTCNA----------------------<u>DKYEKAVDYGFRES**RILAE**G*E*D</u>TCARK*E*KTTLRKSKQKTFSV••••
sAvr1b^{PfHRP}	MRLSFVLSLVVAIGYVVTCNA-------------------<u>FNNNLCSKNAKGLNLNK**RLLHE**</u>TQAHV*DD*AAHHAHHVA*D*TFSV••••
sAvr1b^{Pf1615c}	MRLSFVLSLVVAIGYVVTCNA--------------------<u>SYNKINSSSTYTHS**RILKQ**</u>LEFITL*EE*KTVNALQ*E*MLDDSVTFSV••••

B

C

sAvr1b RXLR2^{Arg9}

D

sAvr1b RXLR2^{TAT}

Figure 6. Functional Replacement of Avr1b Host Targeting Signal with Protein Transduction Motifs and *Plasmodium* Host Targeting Signals.

(A) Sequences of modified Avr1b proteins. PfGBP, PfHRP, and Pf1615c refer to the *Plasmodium* Pf GBP-130, Pf HRPII, and Pf PFE1615c proteins (Bhattacharjee et al., 2006). All nonnative Avr1b sequences are underlined, Avr1b RXLR2 and *Plasmodium* RXLX^{E}/$_{Q}$ motifs are in bold, and acidic residues in the dEER region are in italics. The Avr1b secretory leader was used in all constructs. Details of all constructs are given in Supplemental Table 2 online.
(B) Ratio of blue spots in the presence of *Avr1b*-1 compared with the control, assayed as described in Figure 2. Constructs are as in **(A)**. Averages and SE are from eight pairs of shots.
(C) Secretion and reentry of GFP protein fused to Avr1b protein containing Arg$_9$ in place of RXLR2, expressed in onion cells.
(D) Secretion and reentry of GFP protein fused to Avr1b protein containing the TAT protein transduction signal in place of RXLR2, expressed in onion cells.
In **(C)** and **(D)**, DNA encoding the fusion proteins was bombarded into onion epidermal cells using the Gene Gun without the double-barrel attachment. Cells were photographed 24 h after bombardment.

Table 2. Function of RXLR2 Mutants of Avr1b Assayed by Particle Bombardment

RXLR2 Sequence[a]	Ratio of GUS-Positive Spots[b]		Ablation[c]	P Value[d]	Activity
	rps	Rps1b			
RFLR	1.26 ± 0.07	0.28 ± 0.03	0.78	<0.001	Yes
<u>A</u><u>A</u><u>A</u><u>A</u>	0.93 ± 0.04	0.96 ± 0.05	0	>0.100	No
<u>K</u>FLR	1.04 ± 0.04	0.70 ± 0.04	0.33[e]	<0.001	Partial
<u>Q</u>FLR	0.95 ± 0.03	0.99 ± 0.03	0	>0.100	No
<u>F</u><u>R</u>LR	1.00 ± 0.04	0.98 ± 0.05	0	>0.100	No
RFL<u>Q</u>	0.98 ± 0.07	0.41 ± 0.08	0.58[e]	<0.001	Partial
<u>Q</u>FL<u>Q</u>	1.03 ± 0.05	1.05 ± 0.05	0	>0.100	No
RF<u>A</u>R	0.94 ± 0.03	0.91 ± 0.05	0	>0.100	No
RF<u>V</u>R	0.95 ± 0.05	1.03 ± 0.07	0	>0.100	No
RF<u>RL</u>	1.02 ± 0.04	0.96 ± 0.04	0	>0.100	No

[a] Amino acid sequence of RXLR2 in the wild type and mutants. RFLR is the wild type. Altered residues are underlined.
[b] Ratio of blue spots in the presence of various RXLR2 mutants of *Avr1b*-1 compared with the control empty vector when bombarded onto leaves from *rps* plants (Williams) or *Rps*1b plants (L77-1863). Averages and SE are from 16 pairs of shots.
[c] Ablation calculated as 1 − (Rps1b ratio)/(rps ratio) for ratios significantly different between *rps* and *Rps*1b.
[d] P values comparing results from *rps* and *Rps*1b cultivars were calculated using the Wilcoxon rank sum test.
[e] Ablations for KFLR and RFLQ were significantly different than the wild type (RFLR) with P < 0.001.

motifs were first identified during the *Phytophthora* genome sequence annotation (Rehmany et al., 2005; Govers and Gijzen, 2006), there has been extensive speculation that these motifs are involved in transporting avirulence proteins into host cells (Rehmany et al., 2005; Birch et al., 2006). We have demonstrated here experimentally that the RXLR and dEER motifs do indeed have this function.

As summarized in Figure 7, we first demonstrated that both the RXLR2 and dEER motifs of Avr1b are required for this protein to confer avirulence on *P. sojae* transformants. Next, using a particle bombardment assay, we confirmed that the RXLR2 and dEER motifs are not required to trigger an interaction with the *Rps*1b gene product when the Avr1b protein is synthesized in the soybean cytoplasm. Furthermore, we showed that when Avr1b protein is directed to be secreted out of the soybean cell, the RXLR2 and dEER motifs are once more required for the protein to trigger an interaction with Rps1b, which is consistent with the motifs being required for the Avr1b protein to reenter the soybean cell across the plasma cell membrane. The inferred targeting of Avr1b was supported using GFP fusions. Finally, we showed that fusion of the RXLR-dEER region to GFP enabled the isolated fusion protein to enter soybean root cells in the absence of the pathogen but only if the RXLR and dEER motifs were both intact.

Our findings that the RXLR and dEER motifs are required for Avr1b entry into plant cells are consistent with the finding that RXLR and dEER motifs are required for the *P. infestans* effector Avr3a to enter potato cells (Whisson et al., 2007). Furthermore, our results show that the RXLR and dEER motifs, together with the surrounding sequences, are sufficient for entry into plant cells. Whisson et al. (2007) found that Avr3a protein secreted into the apoplast by *Pectobacterium atrosepticum* could not trigger an interaction with the R3a gene product of potato and concluded that *P. infestans* must be present for Avr3a to enter the plant cell. Two related issues may explain the conflict with our findings. First, the amount of Avr3a secreted by *P. atrosepticum*

may have been insufficient to overcome proteolysis in the apoplast, whereas a much larger amount of protein was present when we added isolated RXLR-dEER-GFP fusion protein directly to soybean roots. Second, both during formation of a *Phytophthora* haustorium, in which the host cell wall but not the plasma membrane are breached, and in our particle bombardment experiments, the secreted effector protein accumulates close to the host plasma cell membrane; this close localization may facilitate efficient transport into the cells.

We have begun to experimentally define the RXLR motif, which has previously been defined principally from sequence alignments of the hypothetical proteins encoded by the Avh genes. These findings are very important in guiding more reliable bioinformatics searches for RXLR effector candidates. We have shown that the Arg at position 1 and the Leu residue at position 3 are essential for function of the motif. A Lys at position 1 allows some function, but significantly less than Arg. However, there is not a strong requirement for the Arg at position 4. Therefore, by functional assays, the oomycete RXLR motif resembles the *Plasmodium* motif (RxLx^E/$_Q$) even more closely than previously noted. The positioning of Arg-1 and Leu-3 within RXLR also is critical because reversing the order of either of the first or the second pairs in the motif residues abolishes function.

Our results also show that the amino acid sequences flanking the RXLR2 and dEER motifs are required in addition to the motifs themselves for the transit of Avr1b into soybean cells (summarized in Figure 8A). Furthermore, our GFP fusion protein experiments showed that the region from residues 33 to 71 (19 amino acids to the left of RXLR2 and 6 amino acids to the right of dEER) were sufficient for protein translocation. A similar observation was made in the case of the *Plasmodium* host targeting motifs. In *Plasmodium*, seven residues upstream of the motifs and 16 residues downstream were required for the targeting function (Bhattacharjee et al., 2006) (Figure 8A). Our results do not indicate which specific flanking sequences are required. However, HMMs constructed from the 10–amino acid residues
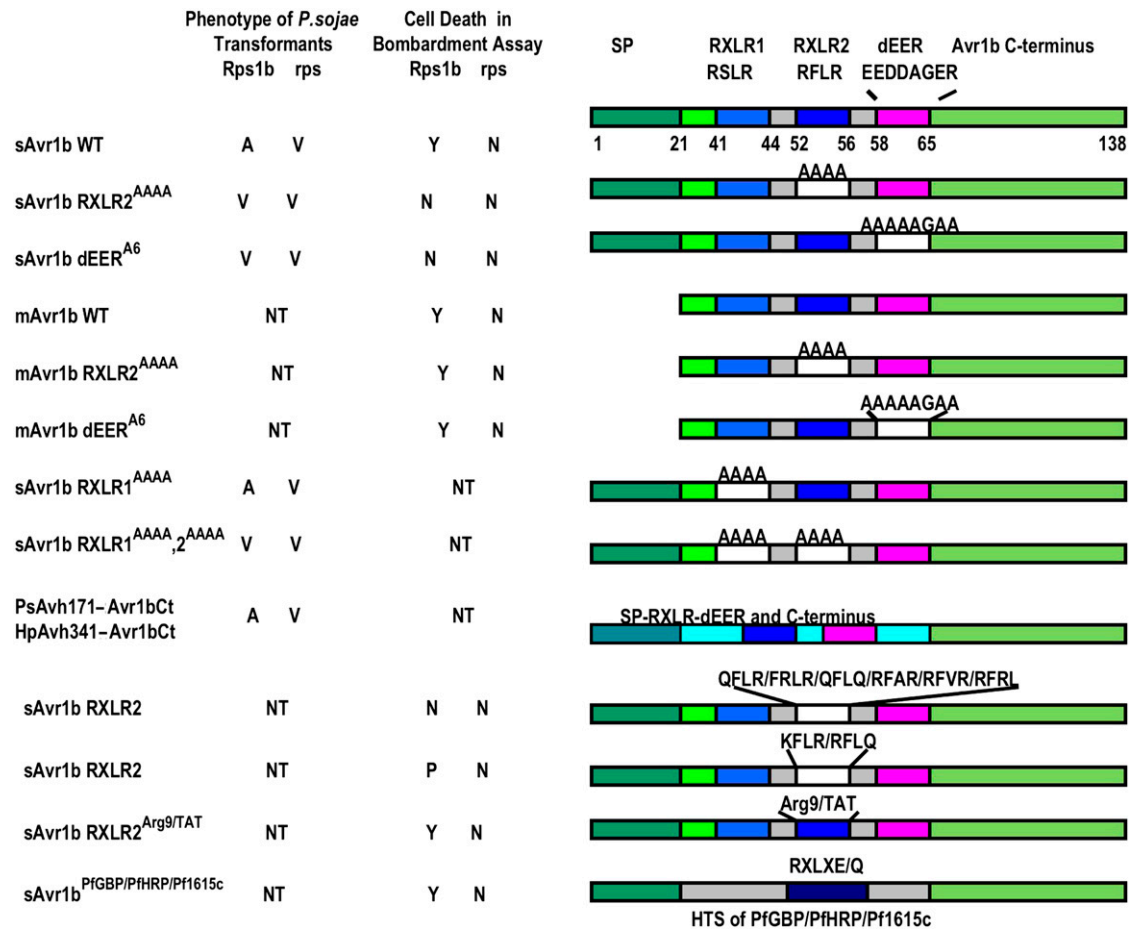
Figure 7. Summary of *Avr1b*-1 Mutations and Their Phenotypes in *P. sojae* Stable Transformants and Soybean Transient Expression Assays.

A, avirulent; V, virulent; NT, not tested; Y, significantly fewer blue (GUS-positive) tissue patches from GUS expression resulting from Avr1b-induced cell death; N, not significantly fewer blue tissue patches; P, partial reduction in blue tissue patches; SP, signal peptide.

flanking the upstream and downstream sides of all *P. sojae* and *P. ramorum* Avh RXLR motifs could clearly separate the RXLR motifs of functional avirulence proteins from RXLR motifs obtained by chance from real or permuted protein sequences (Figure 1D). These findings indicate that reliable bioinformatic searches for RXLR effector candidates should include the use of HMMs to evaluate the sequences flanking putative RXLR and dEER motifs (e.g., Jiang et al., 2008).

One of the most important conclusions from this study is that RXLR-dependent entry of Avr1b does not require the presence of the pathogen. Bacterial plant pathogens have evolved an elaborate mechanism, the type III secretion machinery, for delivering effector proteins into the cytoplasm of plant cells (Plano et al., 2001; Alfano and Collmer, 2004). Nematode plant pathogens deliver effectors into the host cytoplasm through their stylet (Davis and Mitchum, 2005). However, no mechanism has been identified by which filamentous eukaryotic pathogens, such as fungi and oomycetes, deliver effectors to the host cytoplasm. Many oomycete and fungal pathogens, especially those that are biotrophic or hemibiotrophic, form differentiated feeding struc-

tures inside host cells called haustoria (Hahn and Mendgen, 2001; Hardham, 2007). The hyphae displace, but do not penetrate, the plant plasma cell membrane, resulting in the formation of a specialized haustorial interface consisting of the plasma cell membranes of the two organisms, separated by a modified pathogen cell wall (Figure 8) (Hahn and Mendgen, 2001; Hardham, 2007). Haustoria are an obvious site for the release of effector proteins from the pathogen into the plant tissue, as the secreted effectors will be concentrated in close proximity with the plant plasma cell membrane.

PTDs capable of autonomously carrying proteins across plasma cell membranes have been described and characterized in several animal proteins (Joliot, 2005; Langel, 2006), most notably the HIV-1 Tat protein, the *Drosophila* transcription factor antennapedia, the neuropeptide dynorphin, and the defensin Bac7 (reviewed in Langel, 2006; Tomasinsig et al., 2006). Like the targeting sequences of these proteins, the oomycete RXLR motif and the *Plasmodium* Pexel/VTF motif ($RXLX^E/_Q$) are rich in basic and hydrophobic residues. Characterization of the mechanisms by which PTDs transport proteins suggests that an electrostatic
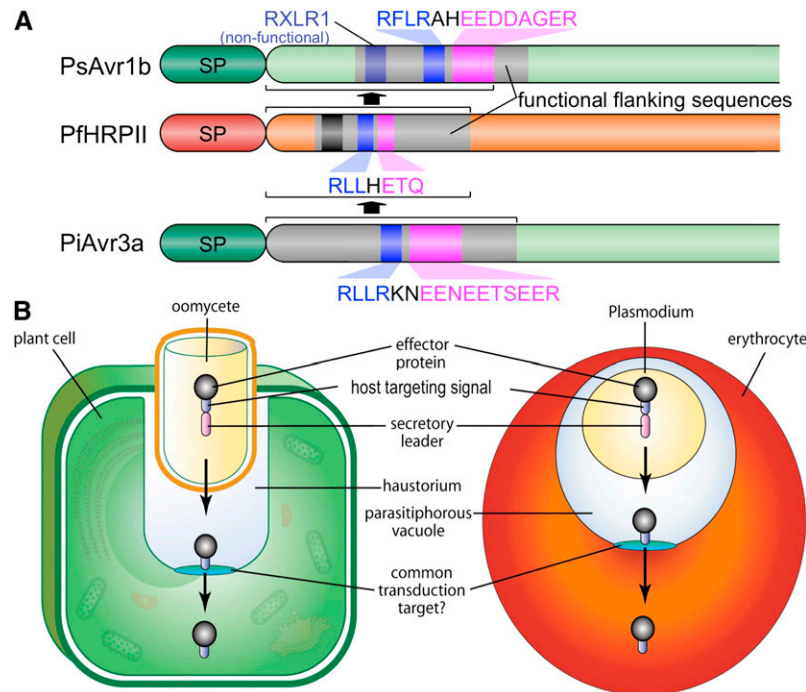
Figure 8. Common Host Targeting Mechanism in Oomycetes and *Plasmodium*.

(A) Features and functional exchange of host targeting signals in *P. sojae* Avr1b, *Plasmodium falciparum* HRPII, and *P. infestans* Avr3a. Common RXL(R) and dEER-like motifs are shown in blue and pink, respectively, and were defined experimentally (this article; Marti et al., 2004; Hiller et al., 2004; Whisson et al., 2007). Flanking regions inferred also to be required are shown in gray. In Ps Avr1b, the flanking regions are defined as the 19 residues upstream and 16 residues downstream of RXLR2 shown to be sufficient for translocation in the GFP fusion experiments. In Pf HRPII, the eight residues upstream and 13 residues downstream were defined experimentally (Bhattacharjee et al., 2006). In Pi Avr3a, the flanking regions are defined by the region tested in *Plasmodium* (Bhattacharjee et al., 2006). The region of Pi Avr3a tested in *Plasmodium* and the region of Pf HRPII tested in *P. sojae* (this article) are shown by the brackets.

(B) Anatomical contexts of oomycete and *Plasmodium* effector entry are similar. The haustorium is a specialized invagination of the plant cell formed by oomycete (and fungal) pathogens. The plant cell wall is pierced during formation of the haustorium, while the oomycete cell wall is retained but differentiates into the haustorial wall. Both the haustorial membrane and the parasitiphorous vacuolar membrane are derived from the host plasma cell membrane during pathogen invasion.

interaction between cationic PTDs and the anionic surface of the plasma membrane leads to transport via a specialized form of endocytosis called macropinocytosis (Snyder and Dowdy, 2004; Kaplan et al., 2005) that occurs in plant cells (Chang et al., 2007) and animal cells. Thus, macropinocytosis is one candidate mechanism by which RXLR-dEER proteins might enter cells. Concordant with this hypothesis, our results show that two of these PTDs can functionally replace RXLR in Avr1b.

The Avr1b protein requires not only the RXLR motif itself but also nonrandom surrounding sequences, including the dEER motif. These surrounding sequences are not enriched in positive and hydrophobic residues but instead are enriched in acidic and hydrophilic residues. Furthermore, our RXLR mutagenesis results show that the presence of basic and hydrophobic residues is not sufficient for RXLR function; instead, the order of the amino acid residues is very important, and very subtle mutations, such as RFLR → RFVR or QFLR, abolish function. Therefore, an alternative hypothesis is that oomycete effectors use a novel mechanism for translocation across the membrane, possibly involving host cell surface machinery (such as a receptor) that is more complex than just the phospholipid bilayer. As summarized in Figure 8A, the *Plasmodium* Pexel/VTF motif also requires surrounding sequences that are enriched in acidic and hydrophilic residues (Bhattacharjee et al., 2006); in fact, the motif is functionally interchangeable with the oomycete RXLR domain in both erythrocytes (Bhattacharjee et al., 2006) and in soybean tissue (this study). Thus, oomycetes and *Plasmodium* both may target host cell surface machinery that is common to plants and vertebrate animals (Figure 8B) but different than that targeted by animal PTDs. A recent study (Bhattacharjee et al., 2008) demonstrated that the *Plasmodium* PTD motif functions by sorting secreted proteins into host cell surface vesicles (Maurer's clefts) that are subsequently internalized, implying the involvement of a cell surface receptor. The targeted machinery, if common, must not only be very ancient but also must serve an irreplaceable function in the host organisms since it must have been preserved against strong negative selection pressure resulting from exploitation by the pathogens. The kingdoms containing oomycetes and *Plasmodium* have a common evolutionary origin within the chromalveolate group (Yoon et al., 2002; Tyler et al., 2006) and so

the RXLR and Pexel/VTF motifs might have a common evolutionary origin. Alternatively, the two pathogens may have acquired a common transduction mechanism through convergent evolution (Figure 8B). If convergent evolution is the explanation, then a much broader array of pathogens might also have acquired this transduction mechanism by convergent evolution, lending considerable importance to characterizing this transduction mechanism.

In fungal pathogens, as discussed in the Introduction, the PtrToxA toxin of *P. tritici-repentis* (Manning and Ciuffetti, 2005) and the RTP1p protein of *U. fabae* (Kemen et al., 2005) have been shown biochemically to enter into host cells, and the products of several avirulence genes have been inferred to do so, namely Avr-Pita (Orbach et al., 2000) of *Magnaporthe oryzae*, AvrL567 (Dodds et al., 2004), AvrM, AvrP4, and AvrP123 (Catanzariti et al., 2006) of *Melampsora lini*, and AVR$_{k1}$ and AVR$_{a10}$ of *B. graminis* f. sp *hordei* (Ridout et al., 2006). So far, no common motif or mechanism has been identified by which these fungal proteins enter plant cells. An RGD vitronectin-like motif has been implicated in PrtToxA transfer into cells (Manning and Ciuffetti, 2005), and the authors suggest that receptor-mediated endocytosis may be involved. Interestingly, an RGD motif overlaps the RXLR motifs of several oomycete effectors (Senchou et al., 2004), and receptors that bind the RGD motifs have been identified (Gouget et al., 2006). The four flax rust Avr gene products share a GxxR motif, but mutagenesis of the motif had no effect on the relevant R gene interactions (Catanzariti et al., 2006). AVR$_{k1}$ and AVR$_{a10}$ of *B. graminis* f. sp *hordei* share a motif ([R/K]VY[L/I]R) with some resemblance to the oomycete RXLR motif, but no functional data are available as to its role (Ridout et al., 2006). The ability to use Avr1b as a reporter protein for entry into plant cells may facilitate the experimental identification of the motifs required for entry of these fungal proteins into plant cells.

METHODS

Plasmids and oligonucleotides used in the study are described in Supplemental Tables 1 and 2 online, respectively.

Phytophthora sojae Isolates and Transformation

P. sojae isolate P7076 (Race 19) (Forster et al., 1994) was routinely grown and maintained on V8 agar (Erwin and Ribiero, 1996). The *P. sojae* transformation procedure was described by Dou et al. (2008) and was kindly provided by A. McLeod and W. Fry (Cornell University) prior to publication. (McLeod et al., 2008).

Characterization of *P. sojae* Transformants

P. sojae transformants were selected that grew well on V8 medium with 50 μg/mL G418 and were cultured in V8 liquid medium for 3 d. The mycelia were harvested, frozen in liquid nitrogen, and ground to a powder for DNA or RNA extraction.

Genomic DNA was isolated from mycelium as described by Judelson et al. (1991). DNA samples were quantified using a Nanodrop ND-1000 spectrophotometer (Thermo Scientific). The presence of *Avr1b*-1 transgenes was verified by PCR amplification from 100 ng genomic DNA using a program of 94°C for 2 min, 30 cycles of 94°C for 30 s, 56°C for 30 s, 72°C for 30 s, and 72°C for 5 min with primers of HamF and HamR (TS1). All the transformed *P. sojae* were double-checked by *Pst*I restriction and/or sequence.

RNA was extracted from each sample using RNeasy plant mini kit (Qiagen) with β-mercaptoethanol added buffer RLT, and genomic DNA was removed using RNase-Free DNase (Qiagen) according to the manufacturer's recommendations. RNA was quantified using a Nanodrop ND-1000 spectrophotometer. *Avr1b*-1 transgene transcription was verified by RT-PCR using the internal primers, Avr1bReF and Avr1bReR (TS1), and *P. sojae* actin was used as the reference.

Phenotypic Assays for Avirulence

Avr1b phenotypic expression was assayed using soybean (*Glycine max*) cultivars HARO(1-7) (rps), Haro13 (Harosoy background, Rps1b), Williams (rps), and L77-1863 (Williams background, Rps1b) (Buzzell et al., 1987). The seed was kindly provided by Terry Anderson (Agriculture Canada). Seedlings were grown in the greenhouse or in a growth chamber (Percival AR-36L) with a program of 24°C at daytime and 22°C at night with a 14-h daylength under fluorescent light (250 μmol photons s^{-1} m^{-2}).

The virulence of each transformant was evaluated using hypocotyl inoculation (Tyler et al., 1995). One to two days after the first primary leaf appeared, the hypocotyl of the soybean was wounded with a short incision and the incision was inoculated with a small piece of V8 agar cut from the edge of a 3-d-old colony. Thereafter, the plants were incubated in a growth chamber under the conditions described above. The numbers of dead and surviving plants were counted 4 d after inoculation and summed over two to five replicates. The differences between the numbers of surviving plants from *rps* and *Rps*1b cultivars were compared using Fisher's exact test (Sokal and Rohlf, 1995). Only the transformants producing a significant difference between rps and Rps1b cultivars were judged as avirulent.

Particle Bombardment Assays

Particle bombardment assays were performed using a double-barreled extension of the Bio-Rad He/1000 particle delivery system (Dou et al., 2008). Analyzing the bombardment data as a ratio between the test and control shots improves the reproducibility of the measurements greatly (Dou et al., 2008).

The avirulence activity of the *Avr1b*-1 constructs was measured as the reduction in the number of blue spots comparing the *Avr1b*-1 + GUS bombardment with the GUS + control bombardment. For each paired shot, the logarithm of the ratio of the spot numbers of *Avr1b*-1 to that of the control was calculated, and then the log ratios obtained from the *Rps*1b and non-*Rps*1b leaves were compared using the Wilcoxon rank sum test (Sokal and Rohlf, 1995).

Bombardment Assays of Onion Bulb Cells with GFP Constructs

Preparation of DNA-particle mixtures was as described above. Five-millimeter hemispherical layers of yellow and white onion bulbs were bombarded without the double barrel attachment under a 26-p.s.i. vacuum, using a rupture pressure of 1100 p.s.i. The onion layers were incubated between 24 and 48 h at 25°C, and then viewed with a Zeiss Axioskop2 Plus microscope using a 480-nm filter for GFP fluorescence. Images were captured using a Qimaging Retiga 1300 camera. To further confirm that the GFP had been secreted out of the onion cells, plasmolysis was performed for 15 min in 0.8 M mannitol and cells were observed in a Zeiss LSM510 laser scanning confocal microscope with an argon laser excitation wavelength of 488 nm.

RXLR-GFP Fusion Protein Expression and Purification

Residues 33 to 71 of Avr1b (VESPDLVRRSLRNGDIAGGRFLRAHEED-DAGERTFSVTD), including the RXLR1, RXLR2, and dEER motifs, were

fused to GFP (see Supplemental Table 2 online), replacing the Arg$_9$ encoding sequences in vector pR9GFP (called pR9 by Chang et al., 2005). pR9GFP, which also adds an N-terminal His$_6$ tag, was derived by Chang et al. (2005) from pTAT-HA provided by Steven Dowdy (Washington University, St. Louis, MO).

C43(DE3) *Escherichia coli* cells containing RXLR-GFP fusion constructs or pR9 were grown in 200 mL of Luria-Bertani medium containing 100 μg/mL ampicillin in a 1-liter baffled flask shaken at 240 rpm at 37°C until reaching an OD of 0.4, at which point the cells were induced by addition of 1 mL of 1 M isopropylthio-β-galactoside (final [5 mM]). After 4 h of further growth at the same conditions, the cells were harvested by centrifugation at 4°C and then stored at −20°C. Visual confirmation of GFP expression was noted by the green color of the bacterial cell pellet.

To extract the GFP fusion proteins, cells were thawed on ice for 20 min, and then 4 mL of lysis buffer (50 mM NaH$_2$P0$_4$, 300 mM NaCl, and 10 mM imidazole, pH 8.0) were added per 1 g of wet cell weight. Lysozyme (Sigma-Aldrich) was added to a final concentration of 1 mg/mL, and then the suspension was incubated for 20 min on ice. Sonication (Branson Sonifier 150D, with double stepped microtip, 3 mm) was done at 300 W at 15-s bursts four times with 15-s cooling periods between each burst. The lysate was centrifuged at 10,000*g* for 30 min at 4°C, and then the supernatant was transferred to a fresh tube and kept on ice until use. Five microliters of each sample was stored for SDS-PAGE analysis.

Protein purification using Ni-NTA affinity chromatography was performed using the QiaExpressionist protocol. Two milliliters of 50% Ni-NTA superflow slurry (Qiagen) was loaded on a column. The column was washed twice with 5 mL of wash buffer (50 mM NaH$_2$P0$_4$, 300 mM NaCl, and 20 mM imidazole, pH 8.0). The protein sample was loaded onto the column, and then the column was washed twice with 10 volumes (10 mL) of wash buffer. The protein was eluted with 4 mL of elution buffer (50 mM NaH$_2$P0$_4$, 300 mM NaCl, and 200 mM imidazole, pH 8.0) into 1-mL fractions. These fractions were pooled and concentrated to 300 μL using a centrifugal protein concentrator (Amicon Centriplus Centrifugal Filter Device MWCO-3kDa) at 13,500*g*. The sample was then mixed with an equal volume of 50 mM MES buffer, pH 5.8. The protein concentration was measured at 280 nm using a nanodrop spectrophotometer (ND-1000) and adjusted to 8 mg/mL. All purified GFP preparations fluoresced normally under UV illumination.

RXLR-GFP Fusion Protein Root Cell Transduction Assay

Root tips were cut into lengths of between 0.5 and 1 cm and then were washed with water. Each root tip was completely submerged in 20 μL of the protein solution (8 mg/mL in 25 mM MES, pH 5.8) in an Eppendorf tube. The samples were incubated overnight at 28°C (~12 h). The roots were then washed in 200 mL of water for 4 h while shaken at 100 rpm on a rotary shaker. The roots were then viewed using a Zeiss LSM510 laser scanning confocal microscope with an argon laser excitation wavelength of 488 nm. For nuclear staining, the roots were stained with DAPI (Sigma-Aldrich) and viewed with a 405-nm filter.

HMM Analysis

Using the program HMMER 2.3.2 (Eddy, 1998) (http://hmmer.janelia.org), an HMM was built from the full set of 765 high-quality candidate effectors identified from the *P. sojae* and *Phytophthora ramorum* genomes by Jiang et al. (2008), using the 10 amino acids on the left side of each RXLR motif together with the 10 amino acids on the right side each RXLR motif. The same procedure was used to build an HMM from a curated list of 191 high-quality candidate effectors from *Hyaloperonospora parasitica* developed at the *H. parasitica* genome annotation jamboree in August 2007 and available at pmgn.vbi.vt.edu. To estimate the significance of HMM scores, all proteins (1240) with a predicted N-terminal signal peptide and the string RXLR located between 30 and 60 amino acids after the signal

peptide cleavage site were obtained by translating the genome sequences of *P. sojae* and *P. ramorum* in all reading frames (Jiang et al., 2008). The sequences of all the putative secreted proteins were permuted (other than the signal peptide), and RXLR-containing sequences were again identified; 639 of the permuted proteins had RXLR strings, indicating that ~639 of the 1240 detected RXLR motifs could be expected by chance (Jiang et al., 2008). The distributions of HMM scores from the set of 1240 real proteins, the 639 permuted proteins and the 765 curated proteins were then calculated. The frequency that a permuted protein received a score between 0 and 5.0 was 0.044. The frequency that a permuted protein received a score better than 5.0 was 0.018.

Accession Numbers

Sequence data from this article can be found in the GenBank/EMBL database under accession number EF681127 (Hp *Avh*341). Accession numbers for sequences already in GenBank are as follows: Ps *Avr1b*-1 (AAM20936), Ps *Avr4/6* (ABS50087), Pi *Avr3a* (CAI72345), Hp *Atr1* (AY842877), and Hp *Atr13* (AY785301).

Supplemental Data

The following materials are available in the online version of this article.

   Supplemental Figure 1. Plasmolysis of Onion Cells Expressing Secreted GFP Fusion Proteins.

   Supplemental Table 1. Oligonucleotides Used for PCR and Plasmid Construction.

   Supplemental Table 2. Description of Plasmids Used.

   Supplemental Table 3. Efficiency of PEG-Mediated *P. sojae* Protoplast Transformation.

REFERENCES

Alfano, J.R., and Collmer, A. (2004). Type III secretion system effector proteins: Double agents in bacterial disease and plant defense. Annu. Rev. Phytopathol. **42:** 385–414.

Allen, R.L., Bittner-Eddy, P.D., Grenville-Briggs, L.J., Meitz, J.C., Rehmany, A.P., Rose, L.E., and Beynon, J.L. (2004). Host-parasite coevolutionary conflict between *Arabidopsis* and downy mildew. Science **306:** 1957–1960.

Anderson, P.A., Lawrence, G.J., Morrish, B.C., Ayliffe, M.A., Finnegan, E.J., and Ellis, J.G. (1997). Inactivation of the flax rust resistance gene M associated with loss of a repeated unit within the leucine-rich repeat coding region. Plant Cell **9:** 641–651.

Armstrong, M.R., et al. (2005). An ancestral oomycete locus contains late blight avirulence gene *Avr3a*, encoding a protein that is recognized in the host cytoplasm. Proc. Natl. Acad. Sci. USA **102:** 7766–7771.

Ballvora, A., Ercolano, M.R., Weiss, J., Meksem, K., Bormann, C.A., Oberhagemann, P., Salamini, F., and Gebhardt, C. (2002). The *R*1 gene for potato resistance to late blight (*Phytophthora infestans*) belongs to the leucine zipper/NBS/LRR class of plant resistance genes. Plant J. **30:** 361–371.

Bhattacharjee, S., Hiller, N.L., Liolios, K., Win, J., Kanneganti, T.D., Young, C., Kamoun, S., and Haldar, K. (2006). The malarial host-targeting signal is conserved in the Irish potato famine pathogen. PLoS Pathog. **2:** e50.

Bhattacharjee, S., van Ooij, C., Balu, B., Adams, J.H., and Haldar, K. (2008). Maurer's clefts of *Plasmodium falciparum* are secretory organelles that concentrate virulence protein reporters for delivery to the host erythrocyte. Blood **111:** 2418–2426.

Birch, P.R., Rehmany, A.P., Pritchard, L., Kamoun, S., and Beynon, J.L. (2006). Trafficking arms: Oomycete effectors enter host plant cells. Trends Microbiol. **14:** 8–11.

Bonello, J.-F., Sevilla-Lecoq, S., Berne, A., Risueno, M.-C., Dumas, C., and Rogowsky, P.M. (2002). Esr proteins are secreted by the cells of the embryo surrounding region. J. Exp. Bot. **53:** 1559–1568.

Bryan, G.T., Wu, K.-S., Farrall, L., Jia, Y., Hershey, H.P., McAdams, S.A., Faulk, K.N., Donaldson, G.K., Tarchini, R., and Valent, B. (2000). A single amino acid difference distinguishes resistant and susceptible alleles of the rice blast resistance gene Pi-ta. Plant Cell **12:** 2033–2046.

Buzzell, R.I., Anderson, T.R., and Rennie, B.D. (1987). Harosoy *Rps* isolines. Soyb. Genet. Newsl. **14:** 79–81.

Catanzariti, A.M., Dodds, P.N., Lawrence, G.J., Ayliffe, M.A., and Ellis, J.G. (2006). Haustorially expressed secreted proteins from flax rust are highly enriched for avirulence elicitors. Plant Cell **18:** 243–256.

Chang, M., Chou, J.C., Chen, C.P., Liu, B.R., and Lee, H.J. (2007). Noncovalent protein transduction in plant cells by macropinocytosis. New Phytol. **174:** 46–56.

Chang, M., Chou, J.C., and Lee, H.J. (2005). Cellular internalization of fluorescent proteins via arginine-rich intracellular delivery peptide in plant cells. Plant Cell Physiol. **46:** 482–488.

Cloutier, S., McCallum, B.D., Loutre, C., Banks, T.W., Wicker, T., Feuillet, C., Keller, B., and Jordan, M.C. (2007). Leaf rust resistance gene *Lr*1, isolated from bread wheat (*Triticum aestivum L.*) is a member of the large psr567 gene family. Plant Mol. Biol. **65:** 93–106.

Dangl, J.L., and Jones, J.D.G. (2001). Plant pathogens and integrated defence responses to infection. Nature **411:** 826–833.

Davis, E.L., and Mitchum, M.G. (2005). Nematodes. Sophisticated parasites of legumes. Plant Physiol. **137:** 1182–1188.

Dodds, P.N., Lawrence, G.J., Catanzariti, A.M., Ayliffe, M.A., and Ellis, J.G. (2004). The *Melampsora lini AvrL*567 avirulence genes are expressed in haustoria and their products are recognized inside plant cells. Plant Cell **16:** 755–768.

Dodds, P.N., Lawrence, G.J., and Ellis, J.G. (2001a). Six amino acid changes confined to the leucine-rich repeat beta-strand/beta-turn motif determine the difference between the P and P2 rust resistance specificities in flax. Plant Cell **13:** 163–178.

Dodds, P.N., Lawrence, G.J., and Ellis, J.G. (2001b). Contrasting modes of evolution acting on the complex *N* locus for rust resistance in flax. Plant J. **27:** 439–453.

Dou, D., et al. (2008). Conserved C-terminal motifs required for avirulence and suppression of cell death by *Phytophthora sojae* effector Avr1b. Plant Cell **20:** 1118–1133.

Eddy, S.R. (1998). Profile hidden Markov models. Bioinformatics **14:** 755–763.

Erwin, D.C., and Ribiero, O.K. (1996). *Phytophthora* Diseases Worldwide. (St. Paul, MN: APS Press).

Feuillet, C., Travella, S., Stein, N., Albar, L., Nublat, A., and Keller, B. (2003). Map-based isolation of the leaf rust disease resistance gene *Lr*10 from the hexaploid wheat (*Triticum aestivum* L.) genome. Proc. Natl. Acad. Sci. USA **100:** 15253–15258.

Förster, H., Coffey, M.D., Elwood, H., and Sogin, M.L. (1990). Sequence analysis of the small subunit ribosomal RNAs of 3 zoosporic fungi and implications for fungal evolution. Mycologia **82:** 306–312.

Forster, H., Tyler, B.M., and Coffey, M.D. (1994). *Phytophthora sojae* races have arisen by clonal evolution and by rare outcrosses. Mol. Plant Microbe Interact. **7:** 780–791.

Futaki, S. (2002). Arginine-rich peptides: Potential for intracellular delivery of macromolecules and the mystery of the translocation mechanisms. Int. J. Pharm. **245:** 1–7.

Gao, H., Narayanan, N.N., Ellison, L., and Bhattacharyya, M.K. (2005). Two classes of highly similar coiled coil-nucleotide binding-leucine rich repeat genes isolated from the *Rps*1-k locus encode *Phytophthora* resistance in soybean. Mol. Plant Microbe Interact. **18:** 1035–1045.

Gouget, A., Senchou, V., Govers, F., Sanson, A., Barre, A., Rouge, P., Pont-Lezica, R., and Canut, H. (2006). Lectin receptor kinases participate in protein-protein interactions to mediate plasma membrane-cell wall adhesions in *Arabidopsis.* Plant Physiol. **140:** 81–90.

Govers, F., and Gijzen, M. (2006). *Phytophthora* genomics: The plant destroyers' genome decoded. Mol. Plant Microbe Interact. **19:** 1295–1301.

Hahn, M., and Mendgen, K. (2001). Signal and nutrient exchange at biotrophic plant–fungus interfaces. Curr. Opin. Plant Biol. **4:** 322–327.

Halterman, D., Zhou, F., Wei, F., Wise, R.P., and Schulze-Lefert, P. (2001). The MLA6 coiled-coil, NBS-LRR protein confers AvrMla6-dependent resistance specificity to *Blumeria graminis* f. sp. *hordei* in barley and wheat. Plant J. **25:** 335–348.

Hardham, A.R. (2007). Cell biology of plant-oomycete interactions. Cell. Microbiol. **9:** 31–39.

Harper, J.T., Waanders, E., and Keeling, P.J. (2005). On the monophyly of chromalveolates using a six-protein phylogeny of eukaryotes. Int. J. Syst. Evol. Microbiol. **55:** 487–496.

Hiller, N.L., Bhattacharjee, S., van Ooij, C., Liolios, K., Harrison, T., Lopez-Estrano, C., and Haldar, K. (2004). A host-targeting signal in virulence proteins reveals a secretome in malarial infection. Science **306:** 1934–1937.

Huang, S., van der Vossen, E.A., Kuang, H., Vleeshouwers, V.G., Zhang, N., Borm, T.J., van Eck, H.J., Baker, B., Jacobsen, E., and Visser, R.G. (2005). Comparative genomics enabled the isolation of the *R*3a late blight resistance gene in potato. Plant J. **42:** 251–261.

Jiang, R.H.Y., Tripathy, S., Govers, F., and Tyler, B.M. (2008). RXLR effector reservoir in two *Phytophthora* species is dominated by a single rapidly evolving super-family with more than 700 members. Proc. Natl. Acad. Sci. USA **105:** 4874–4879.

Joliot, A. (2005). Transduction peptides within naturally occurring proteins. Sci. STKE **2005:** pe54.

Judelson, H., Tyler, B.M., and Michelmore, R.W. (1991). Transformation of the oomycete pathogen, *Phytophthora infestans.* Mol. Plant Microbe Interact. **4:** 602–607.

Kaplan, I.M., Wadia, J.S., and Dowdy, S.F. (2005). Cationic TAT peptide transduction domain enters cells by macropinocytosis. J. Control. Release **102:** 247–253.

Kemen, E., Kemen, A.C., Rafiqi, M., Hempel, U., Mendgen, K., Hahn, M., and Voegele, R.T. (2005). Identification of a protein from rust fungi transferred from haustoria into infected plant cells. Mol. Plant Microbe Interact. **18:** 1130–1139.

Langel, U. (2006). Handbook of Cell-Penetrating Peptides, 2d ed. (Boca Raton, FL: CRC/Taylor & Francis).

Lawrence, G.J., Finnegan, E.J., Ayliffe, M.A., and Ellis, J.G. (1995). The *L6* gene for flax rust resistance is related to the *Arabidopsis* bacterial resistance gene *RPS2* and the tobacco viral resistance gene *N.* Plant Cell **7:** 1195–1206.

Manning, V.A., and Ciuffetti, L.M. (2005). Localization of Ptr ToxA Produced by *Pyrenophora tritici-repentis* reveals protein import into wheat mesophyll cells. Plant Cell **17:** 3203–3212.

Marti, M., Good, R.T., Rug, M., Knuepfer, E., and Cowman, A.F. (2004). Targeting malaria virulence and remodeling proteins to the host erythrocyte. Science **306:** 1930–1933.

Martin, G.B., Brommonschenkel, S.H., Chunwongse, J., Frary, A., Ganal, M.W., Spivey, R., Wu, T., Earle, E.D., and Tanksley, S.D. (1993). Map-based cloning of a protein kinase gene conferring disease resistance in tomato. Science **262:** 1432–1436.

McLeod, A., Fry, B.A., Zuluaga-Duque, A.P., Meyers, K.L., and Fry, W.E. (2008). Toward improvements of oomycete transformation protocols. J. Eukaryot. Microbiol. **55:** 103–109.

Mindrinos, M., Katagiri, F., Yu, G.L., and Ausubel, F.M. (1994). The *A. thaliana* disease resistance gene *RPS2* encodes a protein containing a nucleotide-binding site and leucine-rich repeats. Cell **78:** 1089–1099.

Orbach, M.J., Farrall, L., Sweigard, J.A., Chumley, F.G., and Valent, B. (2000). A telomeric avirulence gene determines efficacy for the rice blast resistance gene *Pi-ta.* Plant Cell **12:** 2019–2032.

Plano, G.V., Day, J.B., and Ferracci, F. (2001). Type III export: New uses for an old pathway. Mol. Microbiol. **40:** 284–293.

Qu, S., Liu, G., Zhou, B., Bellizzi, M., Zeng, L., Dai, L., Han, B., and Wang, G.L. (2006). The broad-spectrum blast resistance gene *Pi9* encodes a nucleotide-binding site-leucine-rich repeat protein and is a member of a multigene family in rice. Genetics **172:** 1901–1914.

Qutob, D., Kamoun, S., and Gijzen, M. (2002). Expression of a *Phytophthora sojae* necrosis-inducing protein occurs during transition from biotrophy to necrotrophy. Plant J. **32:** 361–373.

Rehmany, A.P., Gordon, A., Rose, L.E., Allen, R.L., Armstrong, M.R., Whisson, S.C., Kamoun, S., Tyler, B.M., Birch, P.R., and Beynon, J.L. (2005). Differential recognition of highly divergent downy mildew avirulence gene alleles by *RPP1* resistance genes from two Arabidopsis lines. Plant Cell **17:** 1839–1850.

Ridout, C.J., Skamnioti, P., Porritt, O., Sacristan, S., Jones, J.D., and Brown, J.K. (2006). Multiple avirulence paralogues in cereal powdery mildew fungi may contribute to parasite fitness and defeat of plant resistance. Plant Cell **18:** 2402–2414.

Romer, P., Hahn, S., Jordan, T., Strauss, T., Bonas, U., and Lahaye, T. (2007). Plant pathogen recognition mediated by promoter activation of the pepper *Bs3* resistance gene. Science **318:** 645–648.

Sandhu, D., Gao, H., Cianzio, S., and Bhattacharyya, M.K. (2004). Deletion of a disease resistance nucleotide-binding-site leucine-rich-repeat-like sequence is associated with the loss of the *Phytophthora* resistance gene *Rps4* in soybean. Genetics **168:** 2157–2167.

Senchou, V., Weide, R., Carrasco, A., Bouyssou, H., Pont-Lezica, R.,

Govers, F., and Canut, H. (2004). High affinity recognition of a *Phytophthora* protein by *Arabidopsis* via an RGD motif. Cell. Mol. Life Sci. **61:** 502–509.

Shan, W., Cao, M., Leung, D., and Tyler, B.M. (2004). The *Avr1b* locus of *Phytophthora sojae* encodes an elicitor and a regulator required for avirulence on soybean plants carrying resistance gene *Rps1b.* Mol. Plant Microbe Interact. **17:** 394–403.

Shen, K.A., Chin, D.B., Arroyo-Garcia, R., Ochoa, O.E., Lavelle, D.O., Wroblewski, T., Meyers, B.C., and Michelmore, R.W. (2002). *Dm3* is one member of a large constitutively expressed family of nucleotide binding site-leucine-rich repeat encoding genes. Mol. Plant Microbe Interact. **15:** 251–261.

Slusarenko, A.J., and Schlaich, N.L. (2003). Pathogen profile. Downy mildew of *Arabidopsis thaliana* caused by *Hyaloperonospora parasitica* (formerly *Peronospora parasitica*). Mol. Plant Pathol. **4:** 159–170.

Snyder, E.L., and Dowdy, S.F. (2004). Cell penetrating peptides in drug delivery. Pharm. Res. **21:** 389–393.

Sogin, M.L., and Silberman, J.D. (1998). Evolution of the protists and protistan parasites from the perspective of molecular systematics. Int. J. Parasitol. **28:** 11–20.

Sokal, R.R., and Rohlf, F.J. (1995). Biometry. The Principles and Practice of Statistics in Biological Research. (New York: W.H. Freeman and Company).

Song, J., Bradeen, J.M., Naess, S.K., Raasch, J.A., Wielgus, S.M., Haberlach, G.T., Liu, J., Kuang, H., Austin-Phillips, S., Buell, C.R., Helgeson, J.P., and Jiang, J. (2003). Gene *Rb* cloned from *Solanum bulbocastanum* confers broad spectrum resistance to potato late blight. Proc. Natl. Acad. Sci. USA **100:** 9128–9133.

Srichumpa, P., Brunner, S., Keller, B., and Yahiaoui, N. (2005). Allelic series of four powdery mildew resistance genes at the *Pm3* locus in hexaploid bread wheat. Plant Physiol. **139:** 885–895.

Staskawicz, B.J., Mudgett, M.B., Dangl, J.L., and Galan, J.E. (2001). Common and contrasting themes of plant and animal diseases. Science **292:** 2285–2289.

Tomasinsig, L., Skerlavaj, B., Papo, N., Giabbai, B., Shai, Y., and Zanetti, M. (2006). Mechanistic and functional studies of the interaction of a proline-rich antimicrobial peptide with mammalian cells. J. Biol. Chem. **281:** 383–391.

Torto, T.A., Li, S., Styer, A., Huitema, E., Testa, A., Gow, N.A., van West, P., and Kamoun, S. (2003). EST mining and functional expression assays identify extracellular effector proteins from the plant pathogen *Phytophthora.* Genome Res. **13:** 1675–1685.

Tyler, B., Forster, H., and Coffey, M.D. (1995). Inheritance of avirulence factors and restriction fragment length polymorphism markers in outcrosses of the oomycete *Phytophthora sojae.* Mol. Plant Microbe Interact. **8:** 515–523.

Tyler, B.M. (2002). Molecular basis of recognition between *Phytophthora* species and their hosts. Annu. Rev. Phytopathol. **40:** 137–167.

Tyler, B.M., et al. (2006). *Phytophthora* genome sequences uncover evolutionary origins and mechanisms of pathogenesis. Science **313:** 1261–1266.

van der Vossen, E., Sikkema, A., Hekkert, B.L., Gros, J., Stevens, P., Muskens, M., Wouters, D., Pereira, A., Stiekema, W., and Allefs, S. (2003). An ancient R gene from the wild potato species *Solanum bulbocastanum* confers broad-spectrum resistance to *Phytophthora infestans* in cultivated potato and tomato. Plant J. **36:** 867–882.

Wang, Z.-X., Yano, M., Yamanouchi, U., Iwamoto, M., Monna, L., Hayasaka, H., Katayose, Y., and Sasaki, T. (1999). The *Pib* gene for rice blast resistance belongs to the nucleotide binding and leucine-rich repeat class of plant disease resistance genes. Plant J. **19:** 55–64.

Whisson, S.C., et al. (2007). A translocation signal for delivery of oomycete effector proteins into host plant cells. Nature **450:** 115–119.

Wrather, J.A., and Koenning, S.R. (2006). Estimates of disease effects on soybean yields in the United States 2003 to 2005. J. Nematol. **38:** 173–180.

Wroblewski, T., Piskurewicz, U., Tomczak, A., Ochoa, O., and Michelmore, R.W. (2007). Silencing of the major family of NBS-LRR-encoding genes in lettuce results in the loss of multiple resistance specificities. Plant J. **51:** 803–818.

Yahiaoui, N., Srichumpa, P., Dudler, R., and Keller, B. (2004). Genome analysis at different ploidy levels allows cloning of the pow-dery mildew resistance gene *Pm*3b from hexaploid wheat. Plant J. **37:** 528–538.

Yamane, H., Lee, S.-J., Kim, B.-D., Tao, R., and Rose, J.K.C. (2005). A coupled yeast signal sequence trap and transient plant expression strategy to identify genes encoding secreted proteins from peach pistils. J. Exp. Bot. **56:** 2229–2238.

Yoon, H.S., Hackett, J.D., Pinto, G., and Bhattacharya, D. (2002). The single, ancient origin of chromist plastids. Proc. Natl. Acad. Sci. USA **99:** 15507–15512.